**Final Report**
**TNW2010-05**

**Research Project Agreement No. 65-2781**

# SEISMIC PERFORMANCE AND SMART HEALTH MONITORING OF CONCRETE WITH RECYCLED AGGREGATE

## Part I: Smart Health Monitoring of Concrete with Recycled Aggregate

Pizhong Qiao, Ph.D., P.E.
Professor

**Washington State Transportation Center (TRAC)**
Washington State University
Department of Civil & Environmental Engineering
Pullman, WA 99164-2910

A report prepared for

**Transportation Northwest (TransNow)**
University of Washington
135 More Hall, Box 352700
Seattle, Washington 98195-2700

in cooperation with

**U.S. Department of Transportation**
Federal Highway Administration

August 2010

# TECHNICAL REPORT STANDARD TITLE PAGE

| 1. REPORT NO. | 2. GOVERNMENT ACCESSION NO. | 3. RECIPIENT'S CATALOG NO. | |
|---|---|---|---|
| TNW2010-05 | | | |
| 4. TITLE AND SUBTITLE<br>**SEISMIC PERFORMANCE AND SMART HEALTH MONITORING OF CONCRETE WITH RECYCLED AGGREGATE**<br>**Part I: Smart Health Monitoring of Concrete with Recycled Aggregate** | | 5.REPORT DATE<br>August 2010<br>6. PERFORMING ORGANIZATION CODE | |
| 7. AUTHOR(S)<br>Pizhong Qiao | | 8. PERFORMING ORGANIZATION REPORT NO.<br>TNW2010-05 | |
| 9. PERFORMING ORGANIZATION NAME AND ADDRESS<br>Transportation Northwest Regional Center X (TransNow)<br>Box 352700, 129 More Hall<br>University of Washington<br>Seattle, WA 98195-2700 | | 10. WORK UNIT NO.<br>11. CONTRACT OR GRANT NO.<br>DTRT07-G-0010 | |
| 12. SPONSORING AGENCY NAME AND ADDRESS<br>United States Department of Transportation<br>Office of the Secretary of Transportation<br>1200 New Jersey Ave, SE<br>Washington, D.C. 20590 | | 13. TYPE OF REPORT AND PERIOD COVERED<br>Final Research Report<br>14. SPONSORING AGENCY CODE | |
| 15. SUPPLEMENTARY NOTES | | | |

ABSTRACT

Concrete is one of the most widely used artificial materials in construction, and the consumption of cement and concrete is maintained at a rapid rate of increase. According to the statistics from Europe Cement Society, the world's cement production is about 10 million tons in 1900, but it increased to 6,400 million tons in 1998. Concrete is a composite material, consisting of aggregates and paste. Paste is a continuous phase matrix, in which granular aggregates are embedded. To produce the granular aggregates in concrete, not only a lot of natural resource of stone materials are needed, but also the ecological environment is adversely impacted. On the other hand, when concrete structures reach the limit of their service life, a large amount of old constructions need to be dismantled in addition to natural disasters' destructive effects, leading to a plenty of waste concrete. As a sort of waste produced by demolishing old buildings, waste concrete will result in serious environment pollution and vast resource extravagance if it is not reutilized or recycled.

To protect environment and maintain sustainable development in construction, the technology of recycled concrete is becoming one of the demanding research fields. The frame construction using recycled aggregate concrete (RAC) has been commonly considered in engineering practice, and their ability to resist earthquake loading is important. However, little or no research on seismic performance of the RAC structures has been explored. The objectives of the proposed study are two-fold: (1) to evaluate the seismic performance of RAC structures, and (2) to assess condition and detect damage in RAC using embedded smart piezoelectric sensors/actuators. A combined experimental, theoretical and numerical approach will be considered to evaluate the seismic performance of RAC and develop the condition assessment and damage detection strategy using smart materials.

| 17. KEY WORDS | | 18. DISTRIBUTION STATEMENT | |
|---|---|---|---|
| Aggregates, Recycled materials, Smart structures, Earthquake engineering, Sustainable development | | | |
| 19. SECURITY CLASSIF. (of this report) | 20. SECURITY CLASSIF. (of this page) | 21. NO. OF PAGES | 22. PRICE |
| None | None | 62 | |

# DISCLAIMER

The contents of this report reflect the views of the authors, who are responsible for the facts and the accuracy of the information presented herein. This document disseminated through the Transportation Northwest (TransNow) Regional University Transportation Center under the sponsorship of the Department of Transportation University Transportation Centers Program, in the interest of information exchange. The U.S. Government assumes no liability for the contents or use thereof.

**TABLE OF CONTENTS**

Page

## LIST OF TABLES

## LIST OF FIGURES

Page

## EXECUTIVE SUMMARY

Concrete is one of the most widely used artificial materials in construction, and the consumption of cement and concrete continues to increase. To produce the aggregates in concrete, not only a lot of natural resources of stone or rock materials are needed, but also the ecological environment (in term of a large amount of natural aggregate consumption and cement production) is adversely impacted. On the other hand, many old concrete structures and pavements have reached the end of their service life and need to be replaced. If the old concrete can be better reused as replacement for the aggregate and a portion of the cement in new structures, waste and the impact on the environment in terms of less landfill and savings in natural resources will be reduced. There is also a growing need to utilize the recycled aggregates to replace the natural aggregates as good quality gravel sources are increasingly becoming exhausted.

Recycled aggregates usually present greater porosity and water absorption, lower density, and sometime lower strength than natural aggregates. There is a need to explore the application of smart sensors and actuators in monitoring the properties and health conditions, especially the long term performance, of the recycled aggregate concrete (RAC) structures and evaluate seismic performance of the bridge structures made of RAC. To this end, the objectives of this study are two-fold: (1) to characterize RAC and detect damage and assess condition of RAC using embedded smart piezoelectric sensors/actuators, and (2) to evaluate the seismic performance of RAC structures. In the Phase I (Year 1) of the project, the material characterization of RAC and development of damage detection and health monitoring techniques using smart aggregates are studied.

Both the concrete samples with recycled aggregates (RA) and natural aggregates (NA) were prepared, and their mechanical properties were evaluated and compared. The test results show that the mechanical properties of RAC are usually lower than those of natural aggregate concrete (NAC). The smart aggregates were embedded in concrete beams to serve as either the actuators or sensors, and the elastic wave propagation-based technique was developed to detect the damage (crack) in the RAC beams and monitor the degradation of RAC beams due to the freeze/thaw (F/T) conditioning cycles. The damage detection results and elastic modulus reduction monitoring data demonstrate that the proposed smart aggregates and associated damage detection and monitoring techniques are capable of identifying crack-type damage and monitoring degradation of the RAC structures. Both the RAC and NAC degrade with the increased F/T conditioning cycles. Though the RAC shows a lower reduction percentage of the modulus of elasticity (MOE) from both the dynamic modulus and wave propagation tests at the given maximum F/T conditioning cycle (i.e., 300 in this study), the RAC tends to degrade faster after the 180 F/T cycles. As observed in this study, the material properties and degradation rate of RAC are comparable to those of NAC, thus making the RAC suitable for transportation construction. The findings in material characterization of RAC and development of damage detection and health monitoring techniques using embedded smart aggregates resulted from the Phase I of this study promote the widespread application of recycled concrete in transportation construction and provide viable and effective health monitoring techniques for concrete structures in general.

## INTRODUCTION

### RECYCLED AGGREGATE CONCRETE (RAC)

Due to advantageous properties of concrete (such as its durability, compression strength, fire resistance, lower cost, etc.), it is one of the most extensively used construction materials in the world. In the United States alone, about 260 million cubic meters of ready mixed concrete have been used each year (Kosmatka et al., 2002).

Concrete is a mixture of cement (or a combination of cementitious materials), fine aggregate (sand), coarse aggregate (gravel or crushed stone), and water. Coarse aggregate amounts to about 41% in the bulk of concrete (Fig. 1). Obviously, production of concrete will not only consume a large quantity of energy but also a considerable amount of stone or rock resources.

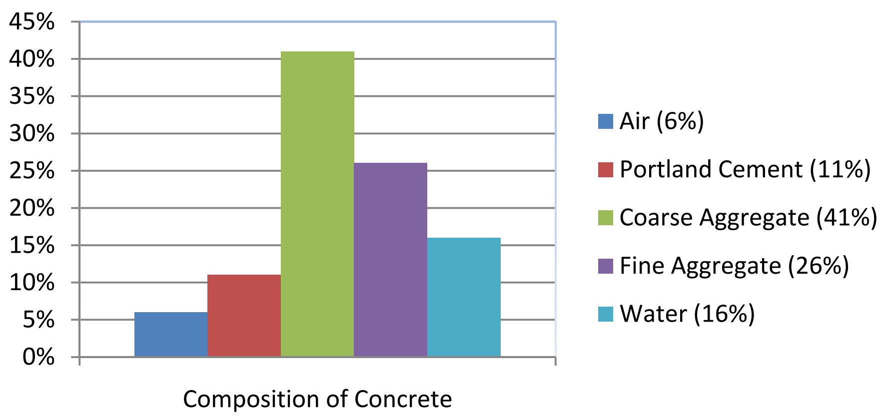


**Figure 1. Composition of Concrete**

The changes of consumption of natural aggregate in the United States are shown in Fig. 2. The use of natural aggregates (includes crushed stone, sand and gravel) has grown significantly from 500 million metric tons in 1900 to 27,800 million metric tons in 1998. Moreover, the consumption of natural aggregates is expected to increase even in the year of 2020 (Kelly, 1998). The ecological environment would be impacted adversely by consuming such a great deal of aggregates as well as by producing cement which accounts for a fair amount in the concrete composition (see Fig. 1). Statistics indicate that the carbon emissions from cement industry make up about 7% of total emissions.

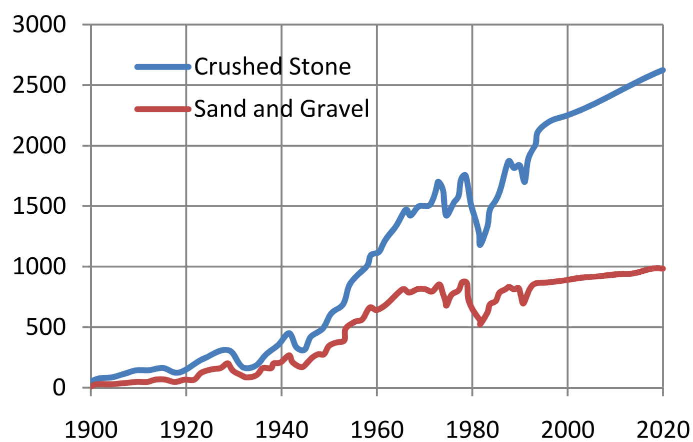


**Figure 2. Consumption of Natural Aggregate in the United States (Kelly, 1998)**

On the other hand, a tremendous number of concrete buildings, bridges and pavements have reached or are approaching the limit of their service life or have been damaged by natural disasters. The structures need to be demolished or renovated, accordingly leading to an enormous quantity of waste concrete. Based on a report in 1999 (Metha, 1999), the European Union countries produced about 200 million tons of building and demolition waste every year, which was estimated to be doubled in the following 10 years.

Waste concrete accounts for a great proportion of the demolition wastes, i.e., approximately 40% (see Fig. 3) (Oikonomou, 2005). The waste concrete caused by demolishing in the United States constitutes about 29% of solid waste (Rogoff and Williams, 1994). It will cost not only a lot of money to dispose of this waste but also precious land resources being used as landfills. Inevitably, the local environment will be polluted and adversely affected.

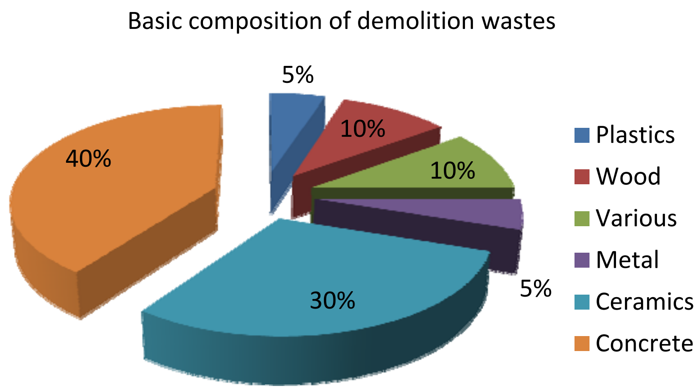


**Figure 3. Basic Composition of Demolition Wastes (Oikonomou, 2005)**

To reduce environmental impacts and cost, the waste resulting from the demolished construction can be recycled and reused in new construction projects. The so-called Recycled Aggregate Concrete (RAC) can be explained as concrete being produced by using crushed waste concrete as its total or partial aggregate. The process of recycling waste concrete is relatively simple, and it includes breaking, removing, and crushing of concrete. There are a variety of benefits in recycling waste concrete rather than treating it as ordinary rubbish. For instance, reusing crushed waste concrete as aggregate in concrete can reduce the landfill space and the need of gravel mining as well as the pollution involved in burying or transporting them. In addition, in many places where the quality aggregates are in a short supply, using RAC in construction is viable and economic.

The use of crushed waste concrete as aggregate for producing new concrete began in Europe at the end of World War II. It was primarily applied in pavement construction. In recent years, the RAC technology has been developed rapidly. In the United States, more than 20 states have used RAC in civil infrastructure. It is anticipated that RAC will be used increasingly in the years to come, because increasing reuse of waste concrete offers an effective green solution (i.e., environmental preservation and effective utilization of resources), reduces the carbon footprint, and increases the sustainability and growth of transportation systems.

## SMART PIEZOELECTRIC MATERIALS

Many sensors and actuators are available for structural health monitoring system. Piezoelectric materials can generate a charge in response to mechanical stimulus (sensor action), or alternatively provide a mechanical strain when an electric field is applied across them (actuator action). The piezo-wafer can be used as actuators to generate the excitations for both the dynamic vibration and wave transmitting. These materials exhibit excellent mechanical strength and have low acoustic impedance, flat response over a wide frequency range, and a broad dynamic response. The piezoelectric materials can be tailored to specific size or application and easily incorporated into other structures, and they are also relatively low in cost (Zou et al., 2000). Repeatability of the experiment is very significant in damage detection, which greatly depends on the repeatability of the excitation forces. In vibration testing, the piezoelectric actuator bonded to or embedded in the structure provides the best repeatability in actuation compared to others, such as impact hammer and electromagnetic shaker (Luo and

Hanagud, 1999). Although the piezoelectric sensors and actuators are effective and promising in structural monitoring, they may not be readily applicable for monitoring the condition of concrete structures. There is a need to evaluate the potential application of piezoelectric sensors and actuators for concrete structures, particularly the structures made of RAC, and develop corresponding health monitoring and damage identification strategies.

# BACKGROUND

In this section, related background information on recycled aggregate concrete (RAC) and concrete health monitoring techniques using piezoelectric materials is reviewed.

## PROPERTIES OF RECYCLED AGGREGATE AND RECYCLED AGGREGATE CONCRETE

### Properties of Recycled Aggregate

The shapes of recycled aggregates (RA) are similar to those of natural aggregates (NA); but the appearances of RA tend to be more angular and rougher, as shown in Fig. 4. The crushing of virgin aggregate particles and the mortar that is adhered to the surfaces of the aggregate are the major causes for more angular and rougher shapes. In addition, the crushing process can lead to numerous micro-cracks in the RA. Generally, RA has a higher water absorption capacity and lower gravity compared to NA.


**Figure 4. Recycled Aggregates (RA)**

Hansen and Narud (1983) reported that the specific gravity of RA is lower than that of NA. According to their experimental data, the specific gravities of RA with a diameter of 4-8 mm and 16-32 mm are 2,340 and 2,490 kg/m$^3$, respectively; while the specific gravities of NA for the same diameter ranges are 2,500 and 2,610 kg/m$^3$, respectively. They also pointed out that RA has a higher water absorption capacity. The absorption ratio of RA is about 8.7% for the diameter of 4-8 mm and 3.7% for the diameter of 16-32 mm, which are many times higher than NA's. The higher water absorption ratio of RA was also observed by several other studies (BCSJ (Building Contractors Society of Japan), 1978; Nixon, 1978; Hasaba et al., 1981; Kreijger, 1983). Topcu and Sengel (2004) further explained that the major causes of high water absorption capacity and low density of RA are due to mortar (old cementitious paste).

**Physical Properties of Recycled Aggregate Concrete**

Traditionally, concrete is considered as a three-phase material composed of aggregate, cementitious paste and the interfacial transition zone (ITZ) between the coarse aggregate and cement paste. It is well known that with normal concrete mixtures the ITZ has a significant effect on the strength of concrete (Nilsen and Monteiro, 1993). But for RAC, it is more complex because the ITZs of NA-cement and RA-cement are both present in RAC, as shown in Fig. 5 (Ryu, 2002). Though there are many factors contributing to the relatively poor mechanical properties of RAC, it is widely recognized that the co-existed ITZs in RAC are one of the main reasons.

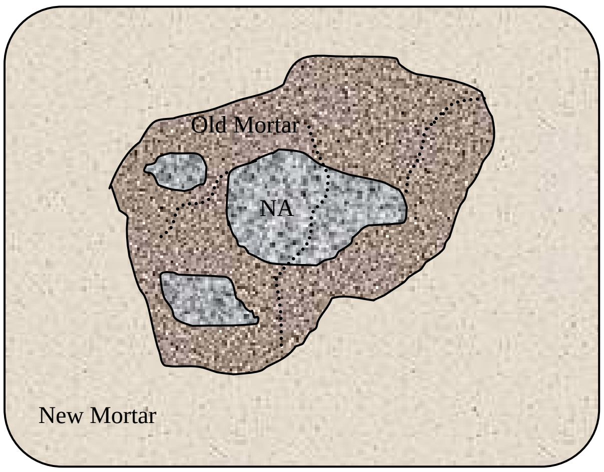


**Figure 5. Interfacial Transition Zones (Solid Lines) and Micro-cracks (Dashed Lines) in RAC**

***<u>Compressive Strength</u>***: Some studies reported that RAC has a higher compressive strength than NAC. Yoda and Yoshikane (1988) and Ridzuan et al. (2001) concluded that RAC has a higher compressive strength which is 8.5% and 2 to 20% higher than that of NAC in their respective experiments. But, most tests showed a decline in the compressive strength of RAC when compared to NAC. Frondistou-Yannas (1977) evaluated the compressive strength of RAC cylinders and found that it is 4 to 14% lower than that of NAC of the same compositions. Ravindrarajah and Tam (1985) also found a reduction in compressive strength of up to 25% of RAC in comparison to that of NAC.

Others considered that the difference of compressive strength between RAC and NAC is very slight, and the compressive strength of RAC is closely related to the properties of waste concrete. Hansen and Narud (1983) studied the compressive strength of RAC as a function of the compressive strength of waste concrete, and they concluded that the compressive strength of RAC is fairly affected by the water-cement ratio of the waste concrete when other factors are essentially identical. Tavakoli and Soroushian (1996) used two sources of crushed concrete pavements from two projects in Michigan as aggregates in their experiment. All the fine aggregates in the RAC and NAC mixtures were 100% natural sands. The test results indicated that RAC had a higher compressive strength if the compressive strength of the waste concrete was higher than that of the control concrete. Limbachiya et al. (2000) used RA to fabricate high strength concrete (7,252 psi (50 $N/mm^2$) or higher). The standard strength testing was carried out at ages 7, 28, 60 and 90 days, and the test results showed that the strength developments with respect to ages for RAC and NAC are similar and RAC with the replacement ratio of coarse RA below 30% has no effect on the strength of concrete, followed by the reduced strength with increasing replacement ratio of RA over 30%.

In summary, the reduction in the compressive strength of RAC can be attributed to the following factors: (1) relatively high porosity of RAC, (2) the weakened areas in the interfacial transition zones (ITZs) of RAC, and (3) lower strength of RA. The contradictory conclusions on the compressive strength with RAC may be due to the differences in the strength of waste concrete, crushing techniques as well as the test methods of experiments considered by different researchers.

***Modulus of Elasticity and Stress-strain Relationship***: Frondistou-Yannas (1977) reported a significant difference (up to 40% lower in RAC) in the modulus of elasticity (MOE) between RAC and NAC and attributed the lower MOE in RAC as a result of lower MOE of RA. Ravindrarajah et al. (1985) reported that the reduction in the MOE of RAC could be up to 30% when compared to NAC. Hansen and Boegh (1985) evaluated both the static and dynamic moduli of RAC and NAC. Both the static and dynamic moduli are reduced about 11% to 28% for RAC and up to 50% when low strength recycled aggregates were used to produce RAC. López-Gayarre et al. (2009) evaluated the influence of quality and the replacement ratio of RA on the MOE of RAC, and they found that the quality of RA is the only influential factor for the MOE of RAC when the replacement ratio of RA does not exceed 50%.

Xiao et al. (2005) investigated the stress-strain relationships of RAC with different replacement ratios of RA (see Fig. 6). In their study, a comprehensive analysis was performed to evaluate the elastic modulus and the peak and ultimate strains of RAC. They found that the replacement ratio of RA does not have a considerable influence on the stress–strain curves of RAC (see Fig. 6).

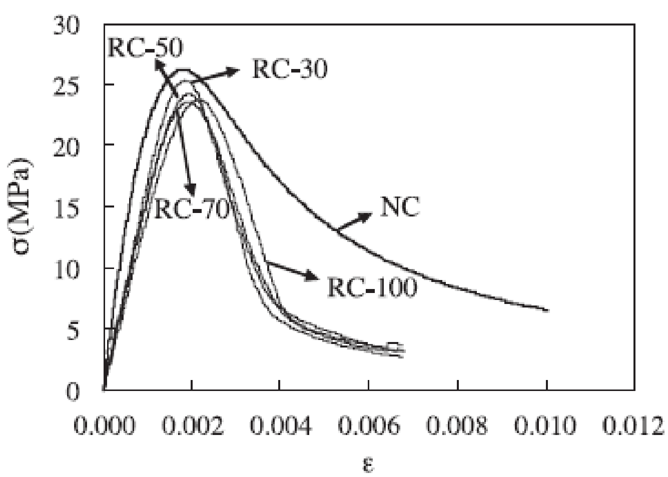


**Figure 6. Stress-strain Diagram of NAC and RAC (Xiao et al., 2005)**

***Flexural and Splitting Tensile Strength***: BCSJ (Building Contractors Society of Japan) (1978) studied the relationship between the flexural strength and compressive strength of RAC and found that the flexural strength is about 1/10 to 1/8 of the compressive strength. Ravindrarajah and Tam (1987) also showed that the flexural strength of RAC is relatively lower, which is about a 10% decrease in comparison with NAC. Salem (1996) applied the empirical equations of different mechanical properties (e.g., the tensile and flexural strength vs. the compression strength) for NAC supplied by ACI code to RAC and evaluated their suitability for RAC. The study found that the conversion function between the tensile and compressive strength was compatible with RAC, but the conversion function between the flexural and compressive strength was conservative. Brito et al. (2004) used three prismatic specimens of 1.97 x 15.75 x 23.62 in. (50 x 400 x 600 mm) to assess the flexural strength of RAC and reported that the flexural strength decreases when the replacement percentage of limestone aggregates with ceramic aggregates increases. Ajdukiewicz and Kliszczewicz (2002) evaluated the splitting strength of RAC based on the pullout method recommended by RILEM and reported that the average decrease of splitting strength is about 20% for the concrete with fully recycled aggregates.

Xiao et al. (2006) proposed two equations to describe the relationship between the flexural ($f_f$)/splitting ($f_{sp}$) strength and compressive strength ($f_{cu}$) by fitting a large number of experimental results available in the literature from 1985 to 2004. The recommended calculation formulas of flexural strength ($f_f$) and splitting strength ($f_{sp}$) for RAC are summarized in Table 1, along with the ones for NAC by the ACI code.

**Table 1. Equations for Flexural and Splitting Tensile Strength**

| Xiao et al. (2006) | ACI Code |
|---|---|
| $f_{sp} = 0.24 f_{cu}^{0.65}$ | $f_{sp} = 0.49 f_{cu}^{0.50}$ |
| $f_f = 0.75 f_{cu}^{0.5}$ | $f_f = 0.54 f_{cu}^{0.5}$ |

**Durability of Recycled Aggregate Concrete**

***Shrinkage and Creep*:** Limbachiya et al. (2000) found that the creep and shrinkage strains increase with the RA content in the mix and the creep effect also increases with reduction in strength. They explained that the increase of creep effect is due to the increased proportion of cement in the RAC. The presence of the attached cementitious paste in RA leads to higher creep and shrinkage in RAC. Hiroshi et al. (2001) used the decompression and rapid release technique to reduce the creep of RAC so that the creep in RAC was reduced to the same level as NAC. Gomez-Soberon (2002) found that the creep increases with the increasing replacement of NA with RA and presented a formula to describe the relation between the creep and porosity ratio. Ajdukiewicz and Kliszczewicz (2002) conducted the creep and shrinkage tests of RAC over a span of one year, and their results showed that the concrete specimens with 100% of RA have about 35-45% higher of shrinkage, while the creep of RAC is about 20% lower than that of NAC. Katz (2003) performed the drying shrinkage tests of RAC and concluded that the shrinkage could be about 0.55-0.80 mm/m at the age of 90 days, whereas the shrinkage of NAC with the same age is only about 0.30 mm/m. Domingo-Cabo et al. (2009) studied the influence of replacement ratios of RA on creep and shrinkage, and they found that the evolution of deformation by shrinkage and creep is similar to that of a conventional concrete with NA. When 100% coarse natural aggregate was replaced by RA, the increases in the creep and shrinkage are about 51% and 70%, respectively.

Shrinkage and creep are of considerable importance if RAC is to be used as viable construction materials. In general, the shrinkage and creep of RAC increase significantly in comparison with NAC, and such increases could be mainly attributed to the old cementitious paste attached to the surface of the natural aggregate in RA and the relatively low elastic modulus of RA. When both the fine and coarse RA are used in the RAC mix, the effect of creep and shrinkage will reach the maximum.

***Water Absorption, Permeability, Carbonation, and Freezing/thawing Resistance*:** Ryu (2002) performed the chloride penetration test to examine the chloride ion permeability of RA. The RAC prisms were made of three types of RA and two water-cement ratios (i.e., 25% and 55%). Test results indicated that the depth of chloride ion penetration in RAC was larger than that of NAC. The mean value of chloride ion penetration depths of all the RAC reached 10.8 mm when the water-cement ratio was 0.55; whereas the mean value of chloride ion penetration depths of NAC was about 9.7 mm.

Buyle-Bodin and Hadjieva-Zaharieva (2002) compared the durability behaviors of RAC and NAC, such as the water absorption, air permeability, and carbonation. Two kinds of RAC were considered: one used sand as its fine aggregate, while the other used the fine RA. The influence of curing conditions was discussed. The test results showed that RAC has nearly 4 times higher of initial absorption, air permeability, and the carbonation rate. When both the fine and coarse RAs were used in the RAC mix, the permeability is about 6.5 times higher than that of RAC with the sand as its fine aggregate and 13 times higher than that of NAC. The results indicated that the curing conditions also have a significant effect on air permeability of RAC, and the air permeability of RAC cured in air increases about 3 times than that cured in water.

Levy and Helene (2004) analyzed the durability of RAC and concluded that when the NA is replaced by 20% of the RA, RAC is likely to perform the same as the reference concrete made of NA in terms of water absorption, total pore volume, and carbonation. However, the water absorption increases when the amount of NA is replaced by RA of more than 20% because the fine and coarse RAs have 6–10 times higher of water absorption rate than that of NA.

Salem et al. (2003) used the relative dynamic modulus of elasticity to assess the resistance of RAC to freezing and thawing (F/T), and their test showed that the use of RA in the replacement of NA reduces the freezing and thawing resistance of concrete due to the relatively high water absorption of RAC. For NAC, adjusting the water-to-cement (w/c) ratio can improve its resistance to freezing and thawing; while it is not so effective for RAC. The use of proper air entraining can significantly enhance the resistance of RAC to freezing and thawing. Zaharieva et al. (2004) studied the frost resistance of RAC, and they found that when the relative length change of RAC reached 500 μm/m, both the compressive and splitting tensile strengths decrease by 10% to 20%; while after 300 F/T cycles, the strengths of RAC are practically exhausted, but the strengths of NAC are usually unchanged even after 300 F/T cycles.

**Structural Behaviors of RAC Members**

Most existing studies on RAC have primarily focused on characterization of their basic material properties and durability. In contrast, there are only limited studies on the behaviors of structures made of RAC.

Sogo et al. (2004) discussed the effects of coarse recycled aggregate type, w/c ratio, and stirrup reinforcement on the shear behavior of RAC beams. The experiment showed the same cracking patterns and failure modes as those of concrete beams made of normal aggregates. While for the beams without stirrup, the shear capacity of RAC beams is lower than that of NAC beams, but they have almost the same shear strength when the stirrup was used. They also observed that decreasing the w/c ratio in RAC could improve the shear strength of the RAC beams.

Yang and Han (2006) evaluated the behavior of RAC-filled steel tubular columns, and the test results showed that the typical failure mode of RAC-filled steel tubular columns was similar to that of normal concrete-filled steel tubular columns. Their study also indicated that the mechanics model developed for the NAC-filled steel tubular columns is still applicable for the calculation of RAC-filled ones.

Corinaldesi and Moriconi (2006) evaluated the behaviors of beam-column joints made of RAC under low cyclic loading, and they compared the seismic performances of joints made of normal concrete, recycled concrete, and recycled concrete mixed with fly ash, respectively. They concluded that due to the low elastic modulus of RAC, the rupture mechanism of RAC beam-column joints is different from a normal concrete joint, and the RAC joints should be designed to be stiffer than the normal concrete joints. Their test also showed that when the fly ash was added to the recycled aggregate concrete, almost the same mechanical performance as the reference normal concrete is resulted.

Xiao et al. (2006) studied the influence of RA replacement ratios in RAC frame on seismic performance using 4½ scale specimens, and they found that the failure patterns of all the specimens are same. The increased replacement ratio of RA reduces the yield, maximum and ultimate loads, but the reductions are quite small. The seismic performance of frames made of RAC is comparable to that of normal concrete frame.

Sato et al. (2007) evaluated the flexural behavior of RAC beams. In their experiment, a total of 37 beams were tested in order to investigate the influences of w/c ratio, tension reinforcement, usage of fine or coarse RAs, curing condition, etc. Based on their extensive experimental study, they observed and concluded that (1) the deflection of RAC beams are larger than that of the normal concrete beams of the same w/c ratio and under the same applied moment; (2) there is no significant difference in crack spacing between the RAC and normal concrete beams; (3) the crack width of RAC beams is larger than that of normal concrete beams; and (4) the ductility of RAC beams is almost the same as the normal concrete beams, so is the ultimate moment. They also evaluated the flexural behavior of RAC beams under sustained load and found that the beams made of fine RA develop many cracks and the deflection of RAC beams cured in a drying condition for one year is almost 2 times larger than that of normal concrete beams.

Ajdukiewicz and Kliszczewicz (2007) compared the behaviors of RAC members (beams and columns) with normal concrete ones. The test results demonstrated that the load bearing capacity of RAC beams is slightly lower (about 3.5% reduction in flexural failure) than that of normal concrete beams; but in the case of shear failure, the capacity of RAC is a bit higher. The deflections of RAC beams are always larger than those of the normal concrete beams. While the test of columns showed that the RAC columns have a better ductility than the normal concrete columns and there are no apparent differences in their failure modes.

In summary, though the performance of structural members made of RAC is relatively poorer than that of their counterparts made of NAC, using crushed waste concrete as aggregates in concrete production is still a feasible solution from their economic and environmental beneficial perspectives. Most of the existing studies on the structural behavior of RAC indicated that there are some differences in the performance and capacity between the RAC and NAC in many aspects, but they may not prevent RAC much from being applied in construction. However, more in-depth studies on structural behaviors of RAC (e.g., their long term and seismic performance) should be conducted, so that the widespread application of RAC can be warranted.

## HEALTH MONITORING OF CONCRETE USING PIEZOELECTRIC MATERIALS

Although RAC is applicable in civil infrastructure, concrete structures are strong in compression but weak in tension which is likely to cause cracking, aging and deterioration, especially for the structures made of RAC. Consequently, an effective health monitoring technique is needed to assess the condition and damage of RAC structures during their service life so that the economic and human life loss can be avoided. There are many nondestructive methods for inspecting concrete structures, such as radiography, acoustic emission, visual inspection, thermal field, etc. But the limitations of these techniques, including accuracy, cost, maneuverability, *in situ* capability, etc., make them difficult and/or incapable of being applied to *in situ* structural health monitoring.

Piezoelectric material, Lead zirconate titanate (called PZT), is a kind of smart materials that has been utilized for detecting the defects in concrete structures in recent years. The PZT patches are small, lightweight and inexpensive, and they can be used as both actuators and sensors by considering their piezoelectric effect. The PZT-based active damage detection methods basically include two types: (1) Impedance-based method; and (2) Elastic wave-based method. In the following, a brief review on damage detection methods of concrete using the above two methods is provided.

**Impedance-based Method**

The impedance-based method utilizes high-frequency structural excitations, typically higher than 20 kHz (Park et al., 2006), and it employs the bonded or embedded PZT patches to capture the changes in mechanical impedance of a structure. Based on the changes in the impedances obtained by the PZT patches, the damages in the structure can be located and identified. Due to its distinct advantages, the electromechanical impedance method has emerged as a powerful health monitoring technique.

Soh et al. (2000) conducted the structural health monitoring of a prototype reinforced concrete bridge under the destructive load. A surface-bonded and self-sensing PZT patch was used to identify the local damage region in its vicinity, in the form of a conductance signature.

Tseng and Wang (2004) used the impedance technique to detect the presence of damage and monitor its progression in concrete. Smart PZT transducers were bonded to the structures to actively provide the local excitation and simultaneously sense the structural dynamic response in high frequency band. The frequency-dependent electric admittance signatures of the piezoelectric transducer were compared with the baseline signatures to determine the status of structural health. The damage was quantified by the root-mean-square deviation (RMSD) index. Two sets of experimental test were performed: one for a concrete beam with progressive damage on the surface, and the other for a concrete beam with progressive damage located in the depth of the specimen. Experimental result showed that the impedance method could effectively detect the presence of incipient damage in concrete beams located at a distance of 360 mm away from the PZT patch. The impedance method could also identify the damage and monitor its progression on the surface as well as in the depth of concrete beams. The progression of damage leads to the continuous increase in the RMSD index.

Based on the equivalent circuit parameters, Wen et al. (2007) embedded the PZT ceramic into concrete blocks monitor the structural health of concrete. After being covered with a layer of rubber, the disc-like ceramic element which works in the thickness mode was first embedded in a cement module and then embedded into concrete structures. Their test showed that the monitoring of both the temperature and stress can be achieved simultaneously by detecting the equivalent circuit parameters.

Yang et al. (2008) employed the structural mechanical impedance extracted from the PZT electromechanical admittance signature as the damage indicator. A comparative study on the sensitivity of the electromechanical admittance and structural mechanical impedance to the damages in a concrete structure was conducted. Their results showed that the structural mechanical impedance is more sensitive to the damage than the electromechanical admittance and thus a better indicator for damage detection.

Shin et al. (2008) presented the application of PZT patches for the strength gain monitoring of concrete. The applicability of the conventional structural mechanical impedance sensing technique, which is normally used for damage detection, was extended to early age concrete monitoring.

**Elastic Wave-based Method**

Wu and Chang (2006a,b) used the high frequency transient stress waves to detect the debonding damage and its location in a reinforced concrete beam based on built-in piezoelectric sensors and actuators in a pitch-catch mode. Three types of tests were conducted: debonding tests in reinforced concrete beams, tensile tests on reinforcement bars, and bending tests of reinforced concrete beams.

Song et al. (2006; 2008) developed the so-called "smart aggregate" based on piezoceramic patches. The proposed smart aggregate was made by embedding a waterproof piezoelectric patch with lead wires into a small cement block (module). The smart aggregates were then mounted in the desired locations in the concrete molds before the casting of the concrete structures took place. The smart aggregates were used to perform three major tasks: early-age concrete strength monitoring, impact detection, and structural health monitoring. The concrete strength development was monitored by observing the high frequency harmonic wave response of the smart aggregates. The impact on the concrete structure was detected by observing the open-circuit voltage of the piezoceramic patch in the smart aggregates. For the structural health monitoring purposes of concrete, a smart aggregate-based active sensing system was designed, and the wavelet packet analysis was considered as a signal-processing tool to analyze the sensor signal. A damage index based on the wavelet packet analysis was used to determine the structural health status.  Their preliminary study demonstrated that the multi-functional smart aggregates have the potential to be applied to comprehensively monitor concrete structures from the earliest age to entire lifetime.

Sun et al. (2006) used the surface-bonded PZT patches for structural health monitoring of a prism concrete beam.  From the velocity of Rayleigh waves and longitudinal waves, the dynamic modulus of elasticity and dynamic Poisson's ratio of the concrete were obtained.  Then, the effect of uniaxial compressive stress and resulting internal cracking of the concrete on the amplitude of the waveforms received by piezoceramic sensors was investigated.  The results confirmed that the piezoceramic sensors and corresponding ultrasonic wave methods had the potential to monitor the cracking and long-term deterioration of concrete structures.

Yan et al. (2009) proposed a smart aggregate-based active sensing approach for structural health monitoring of a concrete shear wall structure.  To evaluate the damage status, the front surface of the shear wall was divided into nine sub-domains.  Then, a sweep sinusoidal signal from 100 Hz to 10 kHz was sent by the smart aggregate actuator.  A wavelet packet-based damage index matrix was proposed to evaluate the damage status in different sub-domains.  The experimental results showed that the proposed smart aggregate-based approach effectively evaluates the damage status in different areas and it is capable of detecting the precautionary point to predict the structural failure.

## PROBLEM STATEMENT

Concrete is one of the most widely used artificial materials in construction, and the consumption of cement and concrete continues to increase.  Concrete is a composite material, consisting of aggregates and paste. Paste is a continuous phase matrix, in which aggregates are embedded. To produce the aggregates in concrete, not only a lot of natural resources of stone or rock materials are needed, but also the ecological environment is adversely impacted. On the other hand, when concrete structures reach the limit of their service life, they need to be dismantled, leading to a plenty of concrete waste. The waste concrete resulting from demolition work in the United States constitutes about 29% of solid waste (Rogoff and Williams, 1994). Concrete waste produced by demolishing old buildings, bridges and pavements results in serious environmental pollution if it is not reutilized or recycled.

From the viewpoints of going green (i.e., environmental preservation and effective utilization of resources), reducing the carbon footprint, and increasing the sustainability and growth of transportation systems, it is beneficial and imperative to reuse concrete waste as recycled aggregates (RA) for new construction. Recycling concrete waste, especially from the demolished transportation and building structures, will lead to reduction in valuable landfill space and savings in natural resources. There is also a growing need to utilize the recycled aggregates to replace the natural aggregates as good quality gravel sources are increasingly becoming exhausted.

The use of recycled aggregate concrete (RAC) acquires particular interest in transportation infrastructure regarding its sustainable development. Recycled aggregates usually have greater porosity and water absorption, lower density, and lower strength than natural aggregates. The construction of highways and bridges using RAC has been considered, and their ability to resist earthquake loading is important. However, little or no research on seismic performance of the bridge structures made of RAC has been explored.  With the advancement of sensor and wireless communication technologies, it is now becoming more viable to monitor and assess the condition of the transportation structures, particularly being built with RAC.  The embedded piezoelectric sensors and actuators in the RAC structures should be capable of monitoring the properties and conditions (including damage), especially the long term performance, of the RAC structures, contributing to smart infrastructure initiatives.  However, the potential and validity of smart materials for effective damage detection and health monitoring of concrete structures have not been fully explored.

## RESEARCH OBJECTIVES

To better evaluate the long term performance and conditions of structures made of recycled aggregate concrete (RAC) and understand the seismic response of RAC bridge structures, the objectives of this study are two-fold: (1) to assess health condition and detect degradation or damage of RAC using embedded smart piezoelectric sensors/actuators, and (2) to evaluate the seismic performance of RAC structures via lab-scale bridge models.  A combined experimental, theoretical and numerical approach is considered to develop the condition assessment and degradation detection strategy using smart materials and evaluate the seismic performance of RAC structures.  In the Phase I (Year 1: 2009-2010) of this study, the condition assessment and degradation/damage detection of RAC using embedded smart piezoelectric sensors/actuators are focused, and the preliminary results are presented in this report.  While the Phase II (Year II: 2010-2011) of the project, if approved and funded, will primarily focus on evaluating the seismic performance of lab-scale bridge models made of RAC.

## METHOD OF ANALYSIS

In this section, the recycled aggregate concrete (RAC) and its mix design, material testing methods, fabrications of smart piezoelectric aggregates and concrete beam samples, and elastic wave-based technique for damage detection and health monitoring of RAC considered in the Phase I study of the project are introduced.

## MATERIALS

### Aggregates

Recycled coarse aggregates were provided by Central Pre-Mix Concrete Company in Spokane, WA, and they contain 30% of virgin (normal) aggregates. The gradations of the recycled coarse aggregates are presented in Table 2. The specific gravities and water absorption of both the recycled aggregate (RA) alone (100% of RA) and virgin aggregate are listed in Table 3. The maximum normal size of RA is about 1-1/4 in. (31.75 mm).

**Table 2. Coarse Recycled Aggregate Gradations (Sieve Analysis)**

| | Recycled Aggregate 1-1/4” |
|---|---|
| Sieves | Cumulative % Passing |
| 1-1/4" | 99.1 |
| 1" | 87.8 |
| 3/4" | 70.3 |
| 5/8" | 56.5 |
| 1/2" | 39.2 |
| 3/8" | 25.2 |
| 1/4" | 5.9 |

Natural fine aggregates were also provided by Central Pre-Mix Concrete Company in Spokane, WA. The fine aggregates meet Class 1 WSDOT Sand requirements. The specific gravity of fine aggregates is also listed in Table 3, and the detailed gradation is given in Table 4.

**Table 3. Specific Gravity and Water Absorption of the 1-1/4" Recycled Aggregates**

| Aggregates | Recycled Aggregate | Virgin Aggregate | Sand |
|---|---|---|---|
| Specific Gravity | 2.32 | 2.68 | 2.65 |
| Absorption | 7.4% | 1.2% | - |

**Table 4. Fine Aggregate Gradation (Sieve Analysis)**

| | Fine Aggregate | |
|---|---|---|
| Sieves | Individual % Retained | Cumulative % Passing |
| 3/8" | 0 | 100 |
| 1/4" | 0.5 | 99.5 |
| #4 | 1.8 | 97.7 |
| #8 | 13.4 | 84.3 |
| #16 | 23.3 | 61 |
| #30 | 18.8 | 42.2 |
| #50 | 24.5 | 17.7 |
| #100 | 13.6 | 4.1 |
| #200 | 1.9 | 2.2 |

## Mix Designs

The standard WSDOT mix design is considered in this study, and the mix design for RAC considered in this study is summarized in Table 5. For comparison purposes, the same mix design with the recycled aggregate (RA) replacing the natural aggregate (NA) is also cast. Thus, the only differences between RAC and Normal or Natural Aggregate Concrete (NAC) are the types of aggregates (RA vs. NA) and the size of coarse aggregates (1-1/4" (31.75 mm) in RA vs. ¾" (19.05 mm) in NA) (see Table 5). The natural fine aggregates (sand) (see Table 4) used in both the RAC and NAC mix designs are same. However, due to the different sizes of coarse aggregates, the cement contents are different, potentially leading to different stiffness and strength.

**Table 5. Mix Designs of RAC and NAC**

| Mixtures | Cement ($lb/yd^3$) | 1-1/4" Recycled Aggregate ($lb/yd^3$) | 3/4" Natural Aggregate ($lb/yd^3$) | Sand ($lb/yd^3$) | w/c | Water (lbs) |
|---|---|---|---|---|---|---|
| RAC | 564 | 1830 | - | 1270 | 0.48 | 270 |
| NAC | 564 | - | 1830 | 1270 | 0.48 | 270 |

**Test Methods**

To characterize the material behavior and quality of RAC, some basic material property (both fresh and hardened) tests (see Table 6) were conducted, including: (1) Air Content, (2) Slump, (3) Compressive strength of concrete, (4) Modulus of elasticity (MOE) of concrete, (5) Flexural strength tests, and (6) Dynamic modulus tests. In addition, as a part of long term health performance evaluation, the rapid freezing/thawing (F/T) cyclic test (ASTM C666) was conducted to accelerate the aging of concrete beam specimens. The material behavior data for the concrete with natural aggregates (i.e., NAC) were also obtained, and they are used to benchmark and compare with RAC.

**Table 6. Fresh and Hardened Property Tests**

| Properties of Concrete | Test Methods |
|---|---|
| Fresh Properties of Concrete | |
| Air content | ASTM C 231/AASHTO T 152 |
| Slump | ASTM C 143/AASHTO T 119 |
| Hardened Properties of Concrete | |
| Compression Strength of Concrete | ASTM C 39/AASHTO T 22 |
| Flexural Strength of Concrete | ASTM C 78/AASHTO T97 |
| Modulus of Elasticity of Concrete | ASTM C 469 |
| Dynamic Modulus | ASTM C215 |
| Rapid F/T Conditioning | ASTM C666 |

## FABRICATION OF SMART AGGREGATES AND CONCRETE SAMPLES

### Smart Aggregates

The smart aggregates are small cement module (cylinder) (about ¾" (19.05 mm) in diameter and ¾" (19.05 mm) in thickness) with embedded thin rectangular PZT patches (plates). The size of the PZT patch used in this study is 0.5 × 0.5 in. (12.7 × 12.7 mm). The PZT patches were first coated with a thin layer of epoxy for waterproofing as shown in Fig. 7. The epoxy-coated PZT patches were then embedded in cement modules and positioned perpendicularly to the cylindrical axis to form the so-called "smart aggregates" (see Fig. 8). These modules were made from a mixture of cement, sand and water (cement:sand:water = 1:1.5:0.48 in weight), and they were cast using a plastic mold (see Fig. 9). The smart aggregates were later embedded into concrete beams to serve as both actuators and sensors for active health monitoring.

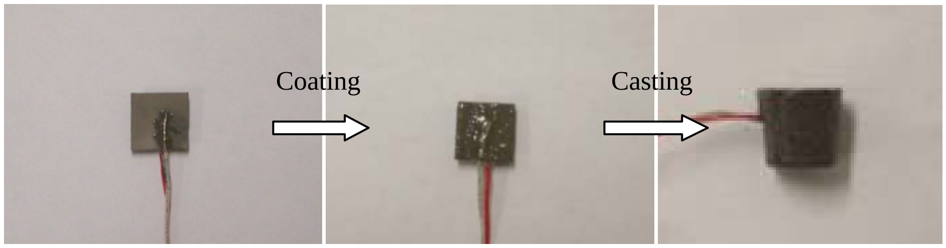


**Figure 7. Fabrication Process of Smart Aggregate**

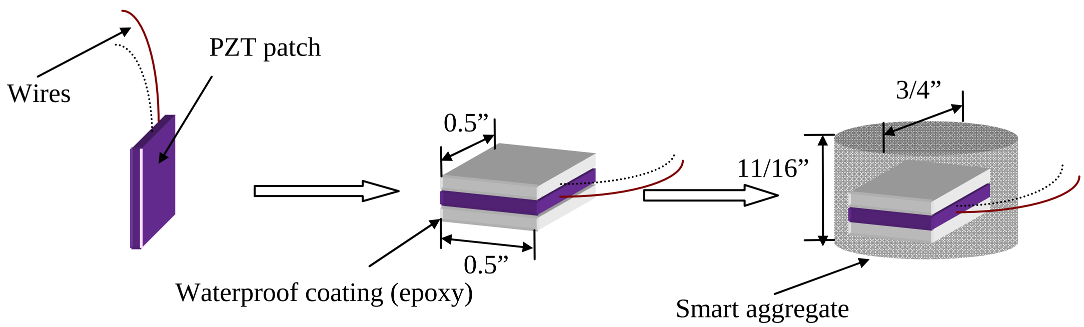


**Figure 8. Schematic of Fabrication Process of Smart Aggregate**

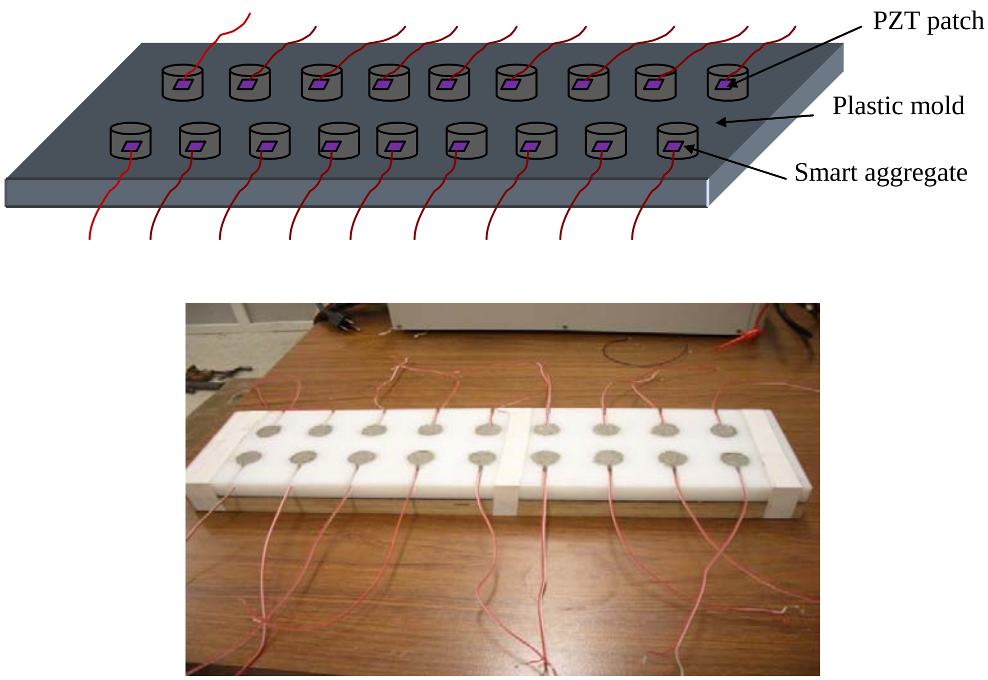


**Figure 9. Plastic Mold for Fabrication of Smart Aggregates**

## Concrete Beam Samples

A total of eight concrete prismatic samples with dimensions of 3 × 4 × 16 in. (76.2 × 101.6 × 406.4 mm) were cast. Three "smart aggregates" were mounted in the mold before casting, and a concrete beam sample with the embedded smart aggregates is shown in Fig. 10. In this study, the four beam samples were made of recycled aggregate concrete (RAC), and the other four serving as a reference were made of natural aggregate concrete (NAC). The mix designs for both RAC and NAC are given in Table 5. All the beam specimens were cured in water at room temperature for 28 days. Three smart aggregates (two were about 1 in. (25.4 mm) from the left and right ends of the beam, and one was located at the center span of the beam, i.e., 8 in. (203.2 mm) from the beam ends) were embedded in each concrete beam sample. The placement of the three smart aggregates is shown in Fig. 10, and the cylindrical axis of smart aggregate was aligned with the beam longitudinal axis.

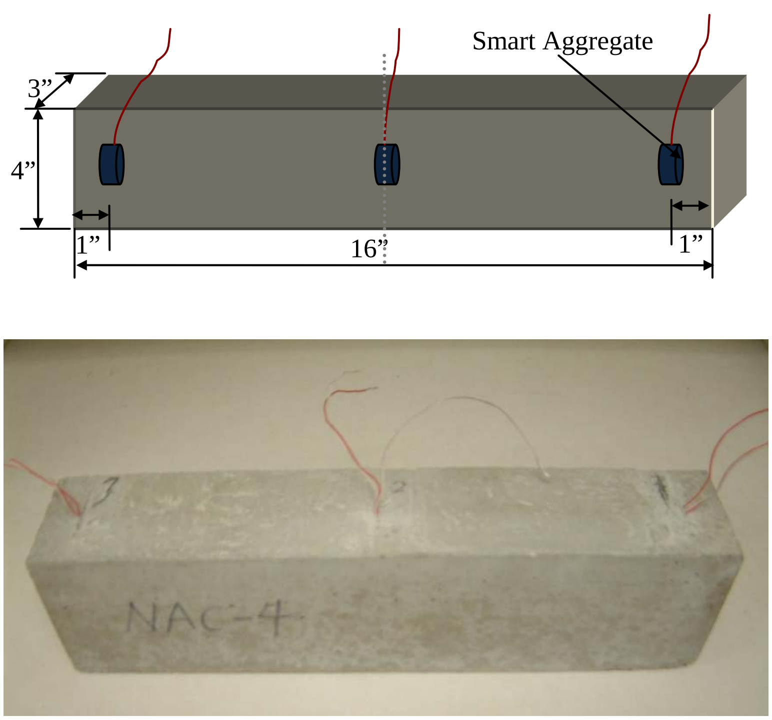


**Figure 10. Concrete Beam Specimen and Placement of Embedded Smart Aggregates**

## DAMAGE DETECTION AND HEALTH MONITORING TECHNIQUES

In this study, the elastic wave propagation-based technique is adopted to develop damage detection and health monitoring techniques for concrete embedded with smart aggregates.

### Damage Detection Technique

In order to detect the damage (crack) inside the concrete, the signal energy $E_s$ of the stress wave is investigated. The signal energy $E_s$ is defined as

$$E_s = \int \left| S(t) \right|^2 dt \tag{1}$$

where $S(t)$ is the signal energy density distribution in time domain measured from the embedded smart aggregates.

It is expected that with the increase of the damage magnitude (e.g., crack depth), the captured stress wave energy level will decrease. As an attempt to quantitatively investigate the extent of damage, the first shear wave package is investigated. This wave package obviously travels from one actuator at one beam end to a sensor at the other beam end in a straight line. The time of flight (*TOF*) of the wave package can be easily identified by the time interval between the peaks of the excitation signal energy and response signal energy. The speed of shear wave ($C_s$) inside the concrete can be predicted by

$$C_s = \sqrt{\frac{E}{2(1+\upsilon)\rho}} \tag{2}$$

where $E$ is the modulus of elasticity (MOE) of concrete; $\rho$ is the density of concrete; $\upsilon$ is the Poisson's ratio of concrete.

From the speed of shear wave, the time of flight (*TOF*) of the first shear wave package can be predicted by

$$TOF = l / C_s \tag{3}$$

where $l$ is the given distance between the actuator and sensor. By comparing the signal energy ($E_s$) of concrete with different magnitudes of damage (e.g., crack depths), the damage in the concrete can be quantitatively assessed; while by evaluating the MOE from the measured *TOF* of concrete at different age (e.g., F/T cycles) (as introduced next), the health condition of the concrete can be monitored.

**Health Monitoring Technique**

The health condition (e.g., degradation) of concrete is monitored by evaluating the change of the modulus of elasticity (MOE) of concrete over time (or at the different F/T cycles in this study). In order to monitor the change of the MOE, the same test procedure as in the damage detection technique is adopted. The *TOF* of the 1$^{st}$ shear wave package is measured to calculate the reduction of MOE caused by the F/T accelerated conditioning or natural aging. Based on Eqs. (2) and (3) and assuming that the Poisson's ratio keep unchanged during the F/T cycling process, the following relationship can be established between the *TOF* and MOE of the concrete samples:

$$TOF \propto \frac{1}{C_s} \propto \frac{1}{\sqrt{E}} \tag{4}$$

Thus, based on the change of the measured *TOF*, the reduction of MOE can be obtained at the different time or F/T cycles, from which the health condition of concrete can be monitored and assessed.

# RESULTS AND DISCUSSION

Both the recycled aggregate concrete (RAC) and natural aggregate concrete (NAC) were evaluated based on results obtained from the tests performed on the concrete in both fresh and hardened states. The damage detection of RAC beams with different crack depths was performed, from which the effect of damage in the RAC beams was quantified. In addition, the health condition (degradation) of RAC beams under the F/T cycles were monitored via the reduction of MOE measured by either the dynamic modulus test or wave propagation test.

## MATERIAL PROPERTY TESTS

### Test Results of Fresh Concrete Properties

Slump and air content tests were performed on fresh concrete for RAC and NAC to evaluate workability and durability properties. The slump test and air content test data for the RAC and NAC mixes are listed in Table 7.

**Table 7. Slump and Air Content Test Data**

| Mixture | RAC | NAC |
|---|---|---|
| Slump (in.) | 4.0 | 2.5 |
| Air Content (%) | 7.5 | 3.0 |

### Test Results of Mechanical Properties

***Compressive Strength and MOE Tests***: ASTM C 39/AASHTO T 22 was adopted to measure the compressive strength of RAC and NAC. ASTM C 469 was used to measure the static modulus of elasticity (MOE). For RAC and NAC, three cylinder specimens of each were casted with 6 in. (152.4 mm) diameter and 12 in. (304.8 mm) height. All the specimens were cured in limewater at the room temperature for 28 days before test. The test was conducted using a hydraulic loading machine (Fig. 11) at a rate of movement of about 0.08 in/min (2.03 mm/min), which is corresponding to a stress rate of 35±7 psi/sec (0.241±0.048 MPa/sec.). The cylinder specimens were first loaded to 40% of its ultimate strength and then unloaded. After that, the displacements and responding loads were recorded to calculate the MOE. Then, the specimens were unloaded again and then reloaded until failure, with all the displacements and load data being recorded.


**Figure 11. Compressive Strength and Modulus of Elasticity (MOE) Tests**

The compressive strength and MOE test results are listed in Table 8. The compressive strength test ensures that the designed/tested concrete mix designs meet the minimum WSDOT 28-days compressive strength requirements of 4,000 psi (27.579 MPa). It should be noted in Table 8 that the MOE data from RAC-1 is excluded from the average as an outlier. It is shown in Table 8 that RAC has lower compressive strength and MOE than those of NAC, although both types of concrete specimens meet the WSDOT 28-days compressive strength requirement of 4,000 psi (27.579 MPa).

**Table 8. Compressive Strength and MOE Test Results**

| Concrete type | Specimen | Compressive strength (psi) | Average (psi) | Young's modulus (x $10^6$ psi) | Average (x $10^6$ psi) |
|---|---|---|---|---|---|
| NAC | NAC-1 | 5,144.7 | 4,844.1 | 3.271 | 3.349 |
| | NAC-2 | 4,745.7 | | 3.396 | |
| | NAC-3 | 4,641.9 | | 3.381 | |
| RAC | RAC-1 | 4,167.5 | 4,158.0 | **3.937** | 2.885 |
| | RAC-2 | 4,340.5 | | 2.940 | |
| | RAC-3 | 3,965.9 | | 2.830 | |

***Flexural Strength Test***: ASTM C 78/AASHTO T97 "Standard Method of Test for Flexural Strength of Concrete (Using Simple Beam with Third-Point Loading)" procedures were followed for measuring the flexural strength of the concrete beam specimens. The concrete beam has a dimension of 4 x 4 x 15 in. (101.6 x 101.6 x 381.0 mm). A span of 12 in. (304.8 mm) was used, which made the height of the beam of 4 in. (101.6 mm), i.e., 1/3 of the span, following the standards. This test was also conducted using the same hydraulic machine (see Fig. 12), with a loading rate of 125-175 psi/min (0.862-1.207 MPa). The flexural strength test results are listed in Table 9. It is shown in Table 9 that RAC has lower flexural strength than NAC.

**Figure 12. Flexural Strength Test**

**Table 9. Flexural Strength Test Results**

| Concrete type | Specimen | Flexural strength (psi) | Average (psi) |
|---|---|---|---|
| NAC | NAC-1 | 687.9 | 691.6 |
| | NAC-2 | 699.2 | |
| | NAC-3 | 687.8 | |
| RAC | RAC-1 | 598.1 | 614.1 |
| | RAC-2 | 627.9 | |
| | RAC-3 | 616.4 | |

**<u>Dynamic Modulus Test (ASTM C215)</u>**

A total of eight concrete prismatic specimens of 3 × 4 × 16 in. (76.2 × 101.6 × 406.4 mm) were prepared for the dynamic modulus test following ASTM C215. Four of them are made of recycled aggregate concrete (RAC), while the other four are made of natural aggregate concrete (NAC). The fundamental transverse frequency was tested to calculate the dynamic modulus of elasticity ($E_{dyn}$) of both the RAC and NAC samples during the curing period and after certain freezing and thawing (F/T) cycles to examine the developing stiffness/strength in the curing and aging (via accelerated F/T condition) stages, respectively. The transverse frequency of the samples were measured by the impact test, where an accelerometer (output signal) was attached to one end of the beam sample, and the test sample was slightly knocked by an impact hammer (input signal) at the approximately central span of the beam sample. The test sample was placed on a thick pad of soft sponge as shown in Fig. 13 to simulate the free condition required by ASTM C215 where the sample is able to vibrate freely in the transverse mode.

**Figure 13. Dynamic Modulus of Elasticity (MOE) Test Setup**

The time domain impulse and response data were automatically recorded by dSPACE data acquisition system and then transferred to the frequency domain using Matlab. The dynamic modulus of elasticity, $E_{dyn}$, can be determined from the fundamental transverse frequency ($n$), mass ($M$), and dimensions ($C$) of the test sample as

$$E_{dyn} = CMn^2 \quad (5)$$

According to ASTM C215, the coefficient $C$ for a prism in Eq. (5) can be obtained as

$$C = 0.9464 \frac{TL^3}{bt^3} \tag{6}$$

where $L$ is the length of the sample; $t$ and $b$ are the thickness and width of the sample, respectively; $T$ is the correction factor which depends on the ratio of the radius of gyration to the length of the specimen and the Poisson's ratio, and it was chosen as $T$ = 1.41 in this study.

All the eight beam samples were cured in the limewater immediately after they were removed from the casting molds. The dynamic MOE tests were conducted in an interval of 3 days during the curing period until 27 days. The variances of the average frequency and dynamic MOE with respect to the curing time for both the RAC and NAC samples are compared in Figs. 14 and 15, respectively. It can be seen from Fig. 14 that the frequency and dynamic MOE gradually increase for both RAC and NAC with the increase of the curing time, indicating that the samples are gaining stiffness and strength. The increased frequency and dynamic MOE during the first half curing time (i.e., the first 15 days) is much larger than those in the rest of the curing time. As a whole, the average frequency and dynamic MOE of RAC are smaller than those of NAC during the curing stage due to the lower mechanical property of the recycled aggregates (RA).

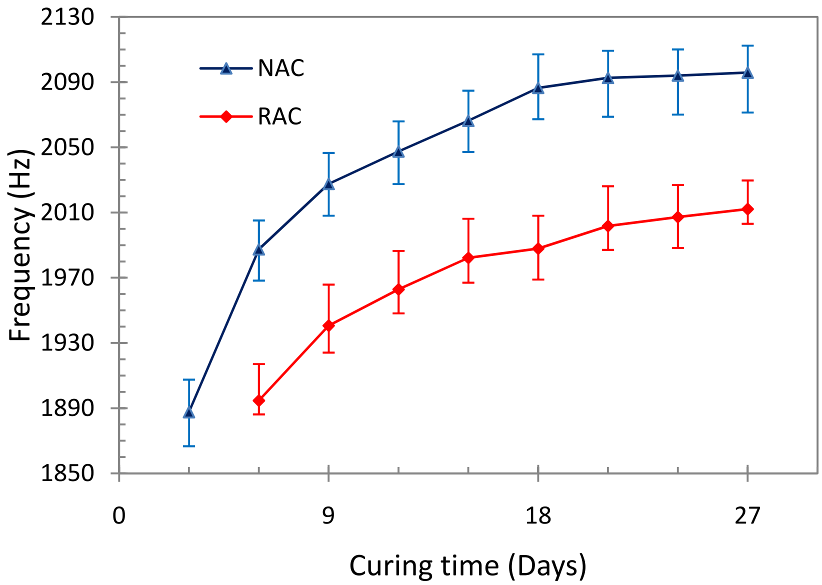


**Figure 14. Variance of Frequency with Respect to Curing Time**

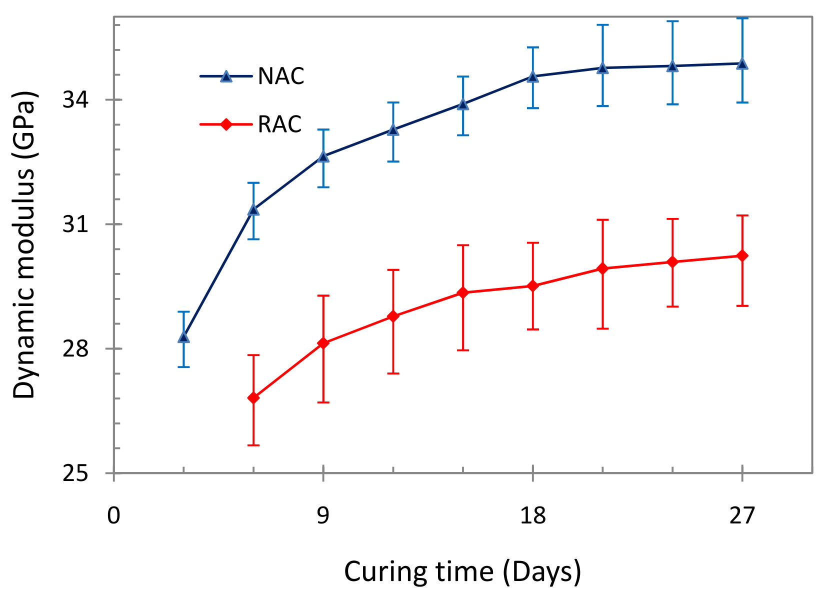


**Figure 15. Variance of Dynamic MOE with Respect to Curing Time**

After 28 days of curing, two samples from each group (i.e., two RAC and two NAC beam samples) were selected for investigating the health condition (e.g., degradation and aging effect) of RAC and NAC under the accelerated freezing and thawing (F/T) condition from 0 to 300 cycles using ASTM C666 (see Fig. 16 for the F/T conditioning machine). The temperature range of every F/T cycle in this study was fixed from 0 to 40$^{o}$F, where the difference between the temperature at the center of a specimen and that at its surface was always checked and controlled not to exceed 50$^{o}$F. The procedure for the F/T conditioning of concrete in ASTM C666 does not explicitly define a point of failure. But a relative dynamic MOE of 60% or less after exposure to 300 F/T cycles is considered failure, and it is implied in ASTM C666.

**Figure 16. Freezing and Thawing (F/T) Machine**

Both the frequency-based (by monitoring the dynamic MOE ($E_d$) changes following the ASTM C215) and wave propagation-based (by evaluating the change of elastic Young's modulus in Eq. (4) via. the *TOF* change) non-destructive monitoring techniques were simultaneously conducted to examine the effect of F/T on the aging of the samples. The variances of the average frequency and dynamic MOE with respect to F/T cycles for both the RAC and NAC samples are compared in Figs. 17 and 18, respectively.  It is obvious that the frequency and the dynamic MOE decrease for both NAC and RAC as the increase of the F/T cycles.

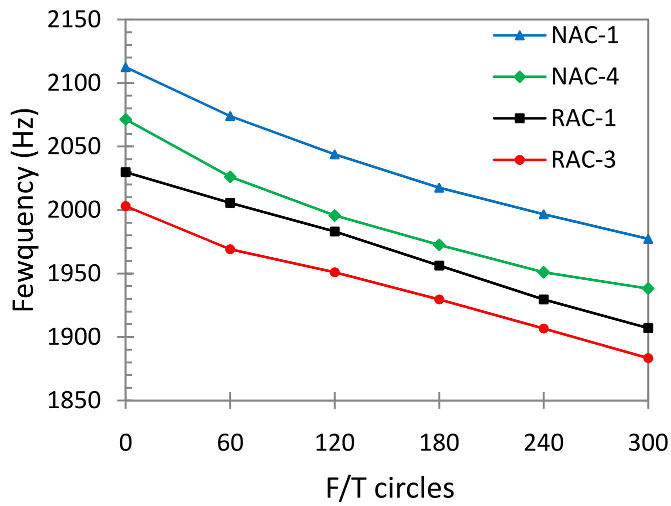


**Figure 17. Variance of Frequency with Respect to F/T Cycles**

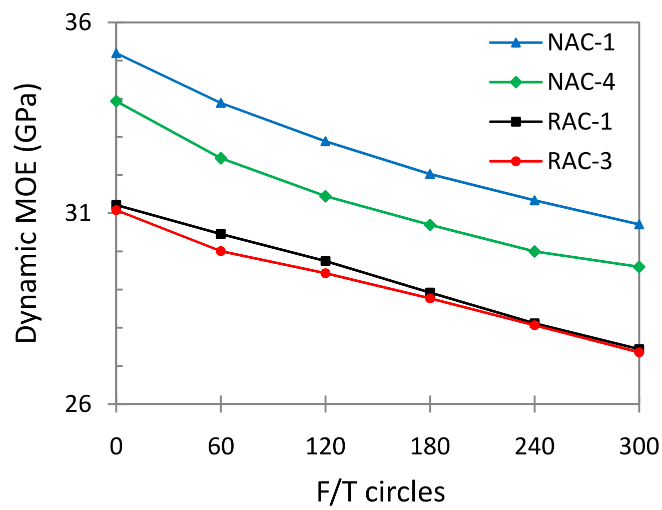


**Figure 18. Variance of Dynamic MOE with Respect to F/T Cycles**

The relative ratios of frequency and dynamic MOE (i.e., the relative values with respect to their original ones) for both the NAC and RAC beams are also shown in Figs. 19 and 20, respectively.  At the 300 F/T circles, the maximum reduced ratios of the frequency are 6.9% and 6.4%, respectively, for the NAC and RAC beams; while the maximum reduced ratios of the dynamic MOE are 12.8% and 12.1%, respectively, for the NAC and RAC beams. From Figs. 19 and 20, it can be observed that after certain F/T circles (180 circles), the slope of the reduced ratio of dynamic MOE for the RAC samples is steeper than that of the NAC samples, indicating that the RAC samples tend to degrade faster than the NAC samples with the increase of F/T cycles. This is mainly due to the high porosity and high water absorption of RAC. But at the F/T cycles of 300, it seems that the reduction ratios of relative dynamic moduli of NAC and RAC are comparable.

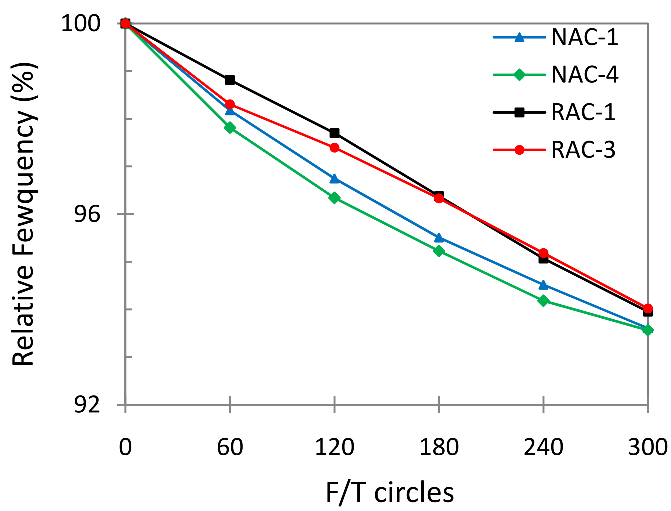


**Figure 19. Variance of Relative Frequency with Respect to F/T Cycles**

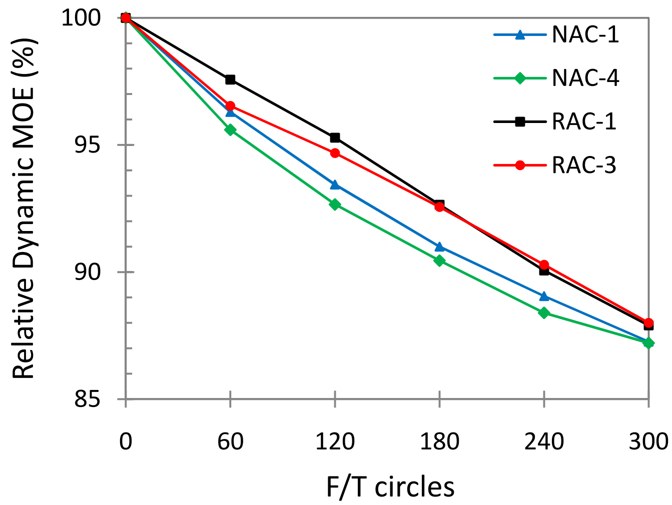


**Figure 20. Variance of Relative Dynamic MOE with Respect to F/T Cycles**

## SMART DAMAGE DETECTION AND HEALTH MONITORING

### Damage Detection of RAC Beams with Embedded Smart Aggregates

***Experimental Setup***: To illustrate the potential of damage detection using smart aggregates, one RAC beam sample embedded with smart aggregates was cut at the quarter span to create a crack-type damage (see Fig. 21) and tested in the laboratory. A crack notch of different depths with a 0.5 in. (12.7 mm) increment (i.e., from 0.5 in. (12.7 mm) to 2.5 in. (63.5 mm)) was artificially induced in the concrete beam by saw-cutting.

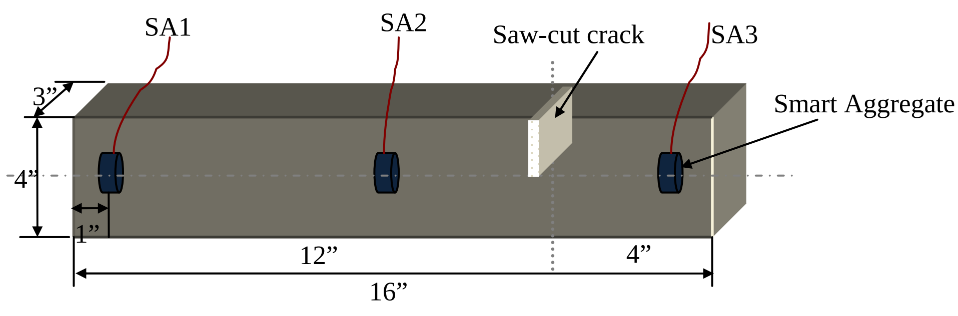


**Figure 21. Artificially-induced Crack Notch in the RAC Beam Sample**

The wave propagation tests were conducted using the smart aggregates embedded at the two ends (one serving as actuator, and the other as sensor) for damage detection. A stress wave was generated by the embedded smart aggregate at one end (e.g., SA1 as shown in Fig. 21), and the response signal was captured by the smart aggregate at the other end (e.g., SA3 as shown in Fig. 21). Since the in-plane dimension of the thin square PZT plate actuator in its plane is much larger than its thickness, the major effect of PZT actuation is perpendicular to the beam length direction. Although both the compressive and shear waves are generated, it is anticipated that the captured shear wave is dominating in terms of signal magnitude. An Agilent 33120A function generator was used to generate the tone burst excitation signal (see Fig. 22). The excitation signal was a 4.5 cycles 100 kHz sine wave windowed by a Hanning window, as shown in Eq. (7) and Fig. 22. A power amplifier was used to amplify the excitation signal in order to drive the PZT actuator inside the smart aggregate. A HP 54603B oscilloscope was used to capture the response signal generated by the PZT sensors at the sampling frequency of 2 MHz. The captured response signal data was then transmitted into a laptop for damage detection analysis. The experimental setup is shown in Fig. 23.

$$S(t) = 0.5(1-\cos(2\pi t\times 100\times 10^3 / 4.5))\times \sin(2\pi t\times 100\times 10^3),\ 0\le t\le 45\times 10^{-6} \qquad (7)$$

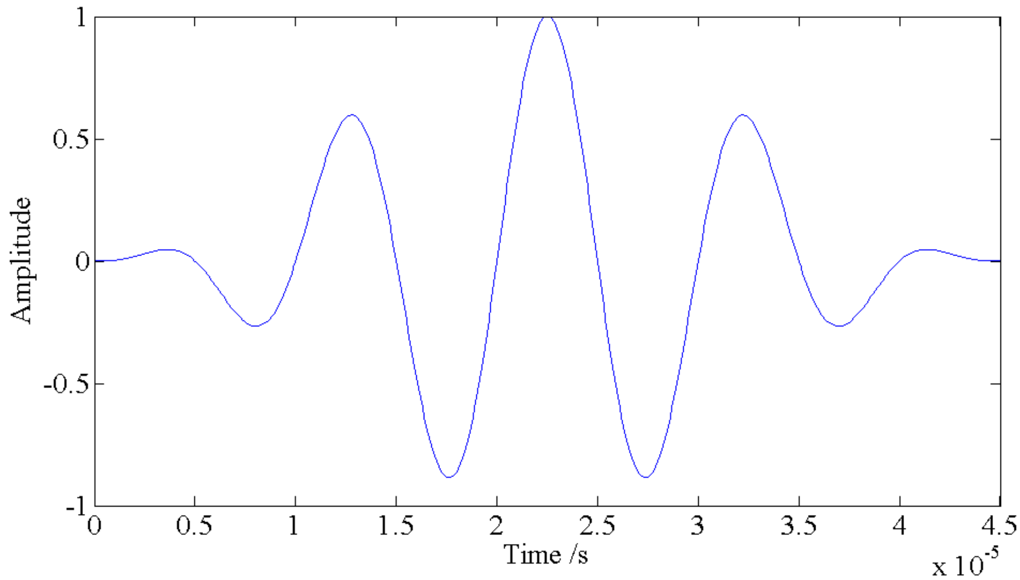


**Figure 22. 100 kHz 4.5 cycles Hanning Windowed Tone Burst**

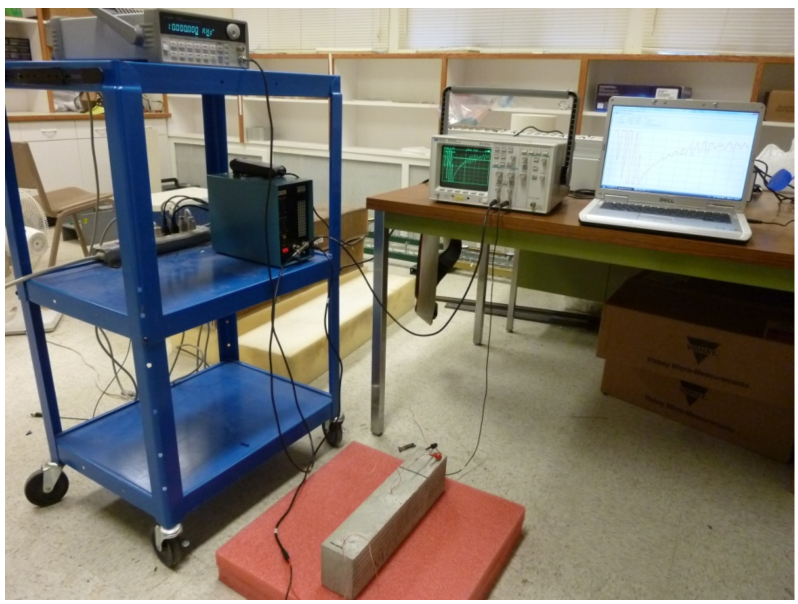

**Figure 23. Experimental Setup for Damage Detection of a RAC Concrete Beam in Smart Structures Lab at WSU**

***Test Results for Damage Detection***: The original signals from the healthy (intact) and damaged RAC beams are shown in Fig. 24. As shown in Fig. 24, the signal captured by SA3 is a combination of stress wave response from PZT sensor and electromagnetic interference (EMI) caused by high voltage excitation signal. In order to eliminate the effect of EMI, an exponential function is used to fit the electrical charge release part of the signal curve. The stress wave response signal is then restored by canceling out the EMI part of the signal from the original signal. The curve fitting is illustrated in Fig. 25. The restored stress wave response signal is shown in Fig. 26.

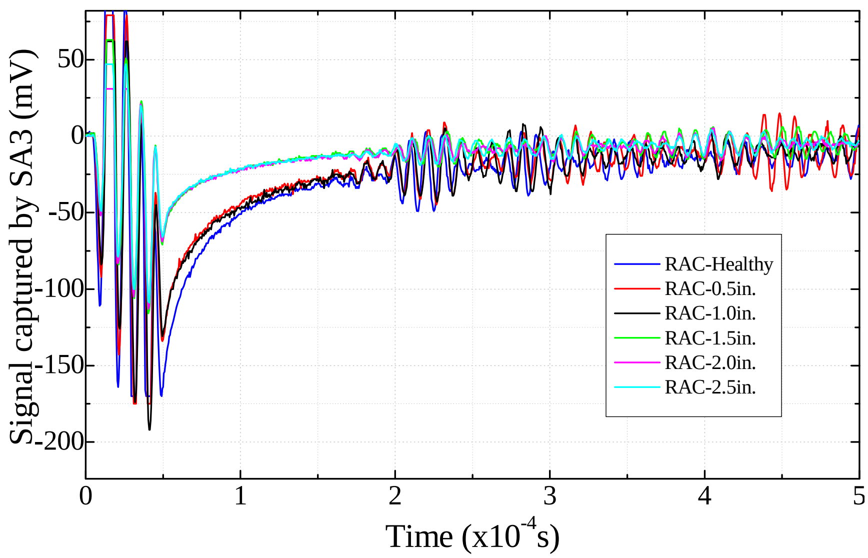


**Figure 24. Original Signals Captured by Smart Aggregate (SA3)**

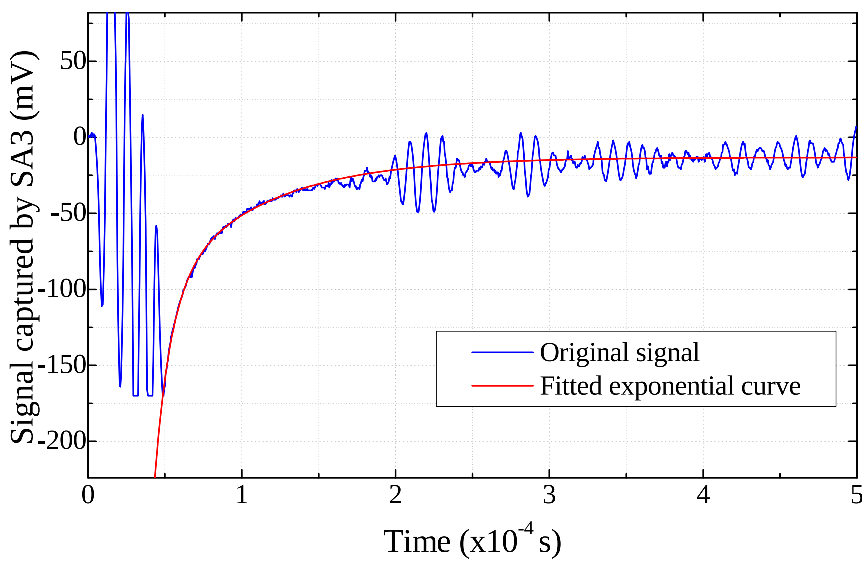


**Figure 25. Original Signal and Fitted Exponential Curve**

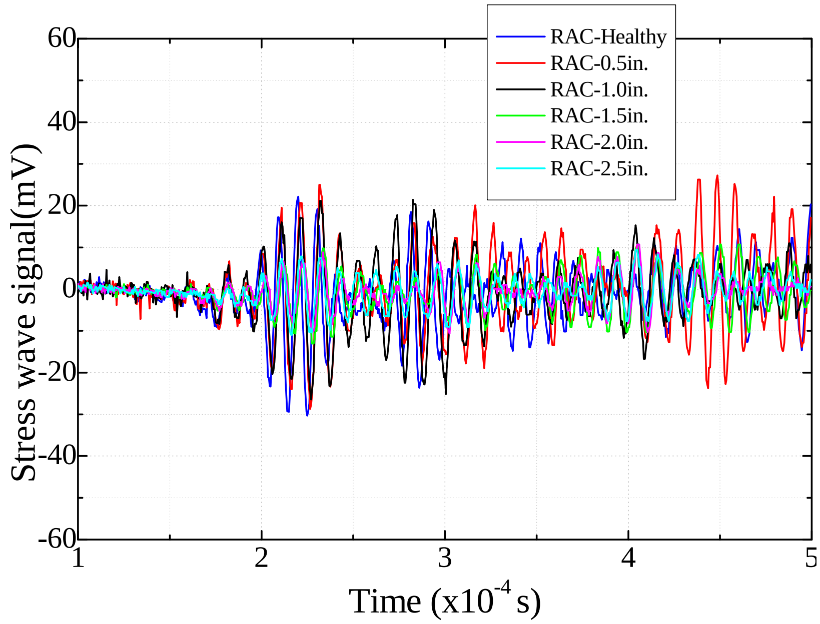


**Figure 26. Restored Stress Wave Signal from the Saw-cut RAC Beam**

In order to detect the damage (i.e., the crack-type notch with different depths in this study) inside the RAC beam, the signal energy $E_s$ of the stress wave in Eq. (1) is investigated. The signal energy density distribution in time domain for the same RAC beam but with different crack notch depths is shown in Fig. 27.

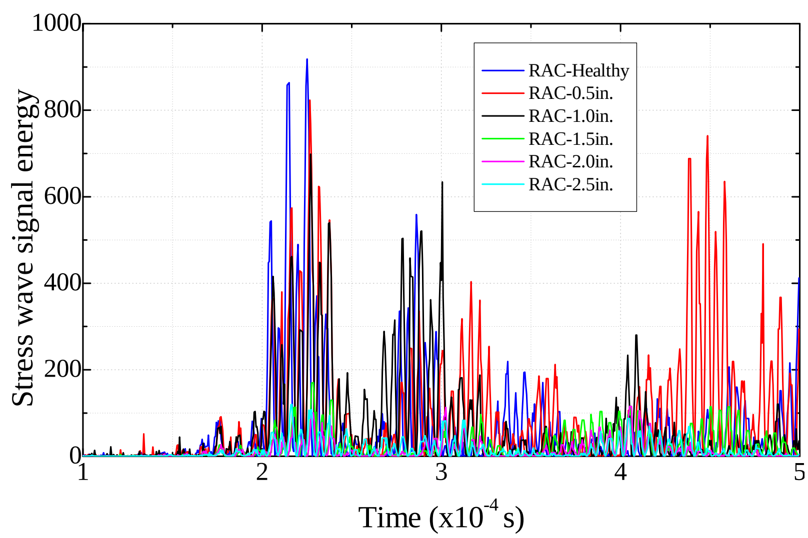


**Figure 27. Stress Wave Signal Energy Density**

As shown in Fig. 27, with the increase of the notch depth, the captured stress wave energy level decreases. As an attempt to quantitatively investigate the extent of the damage, the first shear wave package (approximately from 2.0 to 2.5 x $10^{-4}$ s) was investigated. This wave package obviously travels from the actuator SA1 to the sensor SA3 in a straight line (see Fig. 21). The time of flight (*TOF*) of the wave package was easily identified by the time interval between the peaks of the excitation signal energy and response signal energy. The measured *TOF* for the RAC beam without the presence of crack is 193 μs. The speed of shear wave inside the RAC beam is predicted by Eq. (2) as

$$C_s = \sqrt{\frac{E}{2(1+\upsilon)\rho}} = 1898.7 \text{ m/s} \tag{8}$$

where $C_s$ is the speed of shear wave; in this study, the value of *E* from the MOE test in Table 8 is used, i.e., *E* = 2.885 x $10^6$ psi (19.889 GPa); $\rho$ is the density of RAC, $\rho = 2400 kg/m^3$; $\upsilon$ is the Poisson's ratio, which is assumed to be 0.15.

From the speed of shear wave, the *TOF* of the first shear wave package is predicted as

$$TOF = l / C_s = 0.3556 / 1898.7 = 187 \times 10^{-6} s \tag{9}$$

The predicted (187 μs) and the measured (193 μs) *TOF*s show a close agreement, which confirms that the first wave package is the shear wave propagating from SA1 to SA3 directly.

The total signal energy of the first shear wave package normalized by the signal energy at the healthy state is shown in Fig. 28. It is shown that the shear wave energy captured by SA3 generally decreases with the increase of the notch crack depth in the RAC beam. When the notch depth reaches 1.5 in. (38.1 mm), there is a significant drop of the signal energy because the notch approaches the propagation path of the 1st wave package. Hence, the signal energy of the 1st shear wave package can be used as an index to indicate the existence and roughly the extent of the damage.

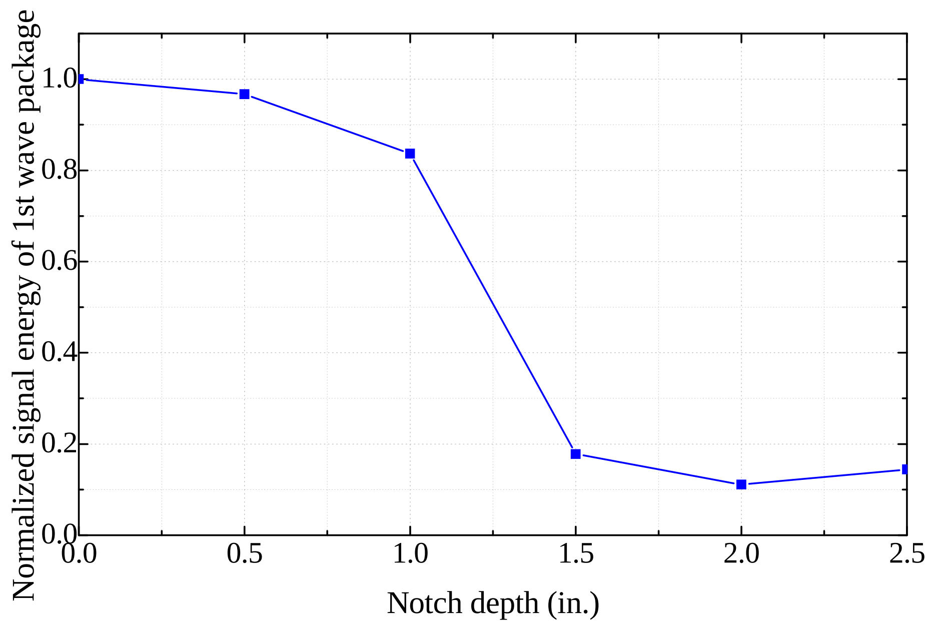


**Figure 28. Normalized Signal Energy of the 1st Wave Package with Different Notch (Crack) Depths**

## <u>Health Monitoring of RAC Beams with Embedded Smart Aggregates</u>

In this section, the two RAC beam samples with the embedded smart aggregates were conditioned in an F/T conditioning machine (see Fig. 16), and their health condition in term of the wave propagation-based modulus of elasticity (MOE), $E_{wave}$ (see Eq. (4)) was monitored with the embedded smart aggregates by the time of flight (*TOF*). The smart aggregates were used to monitor the change of MOE ($E_{wave}$) of the concrete samples at every 60 F/T cycles up to 300 F/T cycles. In order to monitor the change of MOE ($E_{wave}$), the same experimental setup and test procedure as in the damage detection were adopted. The *TOF* of the 1st shear wave package was measured to calculate the reduction of MOE ($E_{wave}$) caused by the F/T cycling process. From Eqs. (2) and (3) and assuming that the Poisson's ratio and density of the RAC beams keep unchanged during the F/T conditioning process, the relationship between the *TOF* and MOE ($E_{wave}$) of the RAC samples in Eq. (4) is used to monitor (or measure) the change of MOE ($E_{wave}$) over the number of F/T cycles.

First, the original signal from SA3 is collected. Then, the same stress wave signal restoration technique as described for damage detection is adopted to restore the stress wave signal. The *TOF* of the 1st shear wave package in the healthy state (i.e., at 0th F/T cycle) is then identified. The delay of the 1st wave package between the 60th F/T cycle (or other higher F/T cycles) and 0th cycle is estimated via a cross-correlation technique. Finally, the ratio between the *TOF*s from the healthy (0 cycles) and conditioned samples (e.g., at 60, 120, 180, 240, and 300 F/T cycles) is used to indicate the change of MOE ($E_{wave}$) during the F/T conditioning process.

As an example, the data from one RAC sample at the 0th and 60th cycle is shown in Fig. 29. The *TOF*s of the healthy and conditioned (at every 60 F/T cycles up to 300 F/T circles) samples and their corresponding MOE ($E_{wave}$) (normalized by the MOE of the healthy state) are listed in Table 10, where the degradation rates as reflected by the MOE ratios of both the RAC and NAC beam samples are compared. The absolute value of MOE based on wave propagation test ($E_{wave}$) and shear modulus ($G_{wave}$) can be obtained as

$$E_{wave} = 2(1+\upsilon)\rho C_s^2 \quad (10)$$

$$G_{wave} = \rho C_s^2 \quad (11)$$

where $C_s$ is computed from Eq. (9) with the measured *TOF* and the known distance (*l*) between the actuator (transmitter) and sensor (receiver).

The variation of the normalized $E_{wave}$ from 0 to 300 cycles is also shown in Fig. 30. As shown in Table 10, the normalized MOE (i.e., the MOE ratio) obtained from the wave propagation test decreases as the number of F/T cycles increases, demonstrating that both the RAC and NAC samples degrade with the F/T conditioning cycles. At the F/T cycles of 300, the reduced normalized $E_{wave}$ are 11.6% and 8.9%, respectively, for the NAC and RAC samples, which are consistent with the dynamic modulus reduction observed in the dynamic tests (see Fig. 20). Though the RAC samples have a smaller percentage of the normalized $E_{wave}$ reduction compared to that of NAC, the RAC samples tend to degrade faster after the 180 F/T cycles (see the steeper slope of RAC after 180 F/T cycles in Fig. 30(c)). The consistency of test results between the frequency (dynamic modulus)-based and wave propagation-based tests demonstrates that the smart aggregates and associated wave propagation-based health monitoring technique are capable of monitoring degradation process in the RAC beams. More important, the wave propagation-based health monitoring technique with embedded smart piezoelectric aggregates as either actuators or sensors has the potential for in situ condition assessment.

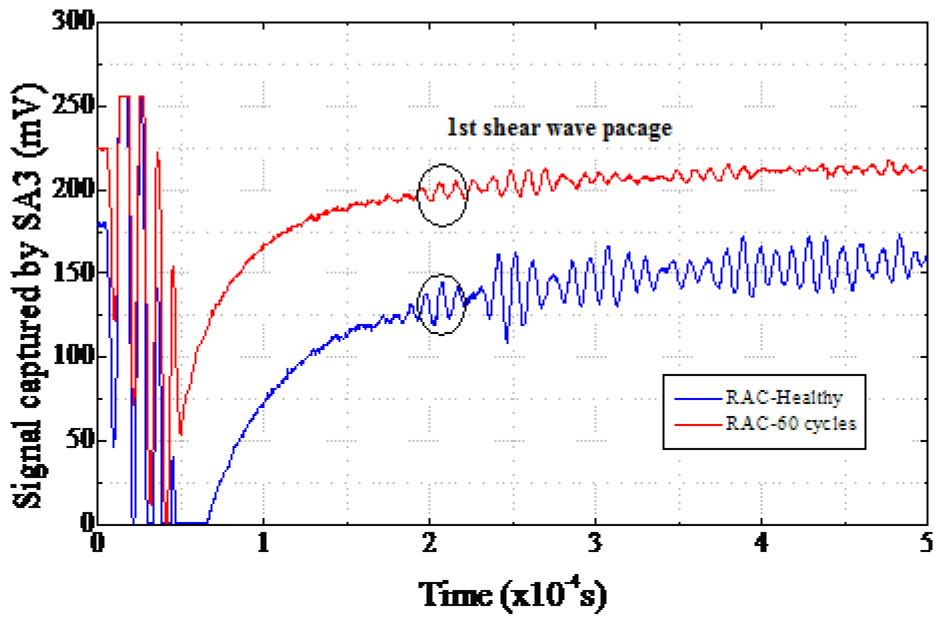


**Figure 29. Original Signals of RAC Sample with 0 cycles and 60 cycles**

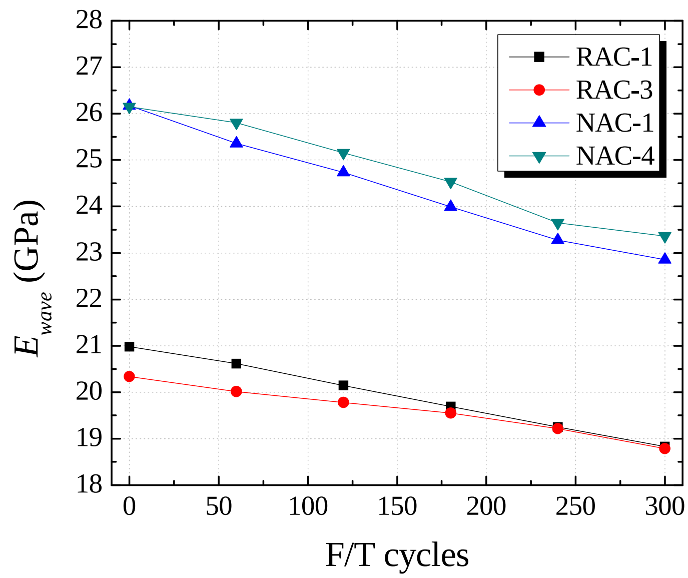


(a) Wave Propagation-based MOE ($E_{wave}$)

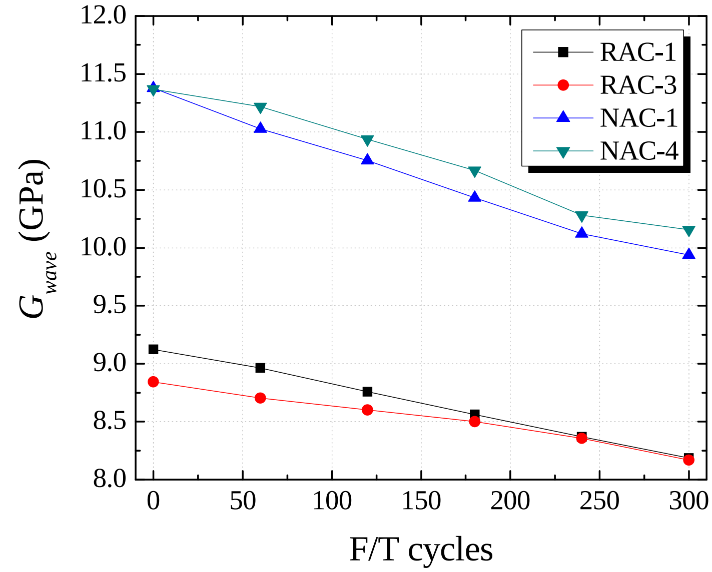


(b) Wave Propagation-based shear modulus ($G_{wave}$)

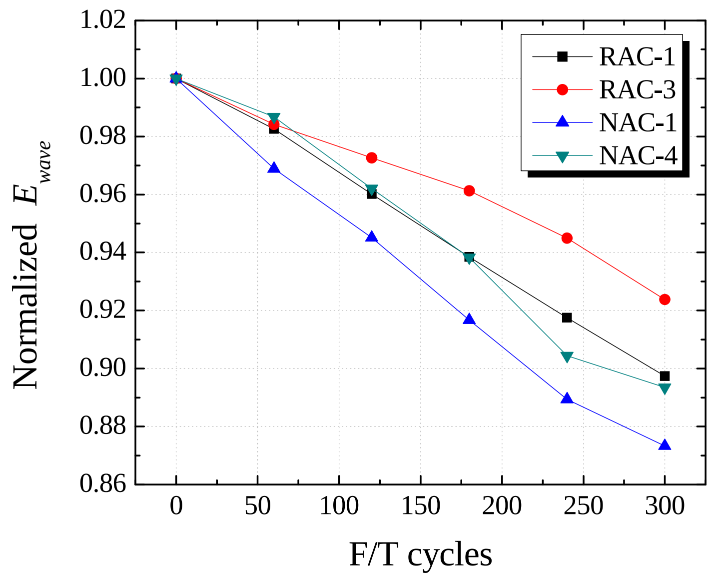


(c) Normalized $E_{wave}$

**Figure 30. Change of Wave Propagation-based MOE with Respect to F/T Cycles**

**Table 10. *TOF*s and Variations of Wave Propagation-based MOE**

| Samples | F/T cycles | TOF ($\times 10^{-6}$ s) | Density ($kg/m^3$) | $E_{wave}$ (GPa) | $G_{wave}$ (GPa) | Normalized $E_{wave}$ |
|---|---|---|---|---|---|---|
| RAC-1 | 0 | 178.0 | 2.286 | 20.982 | 9.123 | 1.000 |
| | 60 | 179.5 | 2.284 | 20.618 | 8.964 | 0.983 |
| | 120 | 181.5 | 2.282 | 20.145 | 8.759 | 0.960 |
| | 180 | 183.5 | 2.280 | 19.691 | 8.562 | 0.939 |
| | 240 | 185.5 | 2.278 | 19.251 | 8.370 | 0.918 |
| | 300 | 187.5 | 2.276 | 18.830 | 8.187 | 0.897 |
| RAC-3 | 0 | 180.0 | 2.266 | 20.338 | 8.843 | 1.000 |
| | 60 | 181.0 | 2.255 | 20.017 | 8.703 | 0.984 |
| | 120 | 182.0 | 2.253 | 19.780 | 8.600 | 0.973 |
| | 180 | 183.0 | 2.251 | 19.552 | 8.501 | 0.961 |
| | 240 | 184.5 | 2.249 | 19.218 | 8.356 | 0.945 |
| | 300 | 186.5 | 2.247 | 18.789 | 8.169 | 0.924 |
| NAC-1 | 0 | 162.0 | 2.362 | 26.170 | 11.378 | 1.000 |
| | 60 | 164.5 | 2.359 | 25.357 | 11.025 | 0.969 |
| | 120 | 166.5 | 2.358 | 24.733 | 10.753 | 0.945 |
| | 180 | 169.0 | 2.356 | 23.991 | 10.431 | 0.917 |
| | 240 | 171.5 | 2.354 | 23.277 | 10.121 | 0.889 |
| | 300 | 173.0 | 2.352 | 22.855 | 9.937 | 0.873 |
| NAC-4 | 0 | 161.0 | 2.330 | 26.146 | 11.368 | 1.000 |
| | 60 | 162.0 | 2.328 | 25.802 | 11.218 | 0.987 |
| | 120 | 164.0 | 2.326 | 25.155 | 10.937 | 0.962 |
| | 180 | 166.0 | 2.324 | 24.533 | 10.666 | 0.938 |
| | 240 | 169.0 | 2.322 | 23.646 | 10.281 | 0.904 |
| | 300 | 170.0 | 2.321 | 23.361 | 10.157 | 0.894 |

# CONCLUSIONS AND RECOMMENDATIONS

In the Phase I (Year I) of the project, the goal is to characterize material properties of recycled aggregate concrete (RAC) and develop damage detection and health monitoring techniques using smart aggregate. A comprehensive literature search was first conducted. Based on the literature review, it concluded that the mechanical and durability properties of RAC are usually lower than those of its counterpart - natural aggregate concrete (NAC), due to low density, high porosity, and high water absorption of the recycled aggregates (RA), and there are only limited studies in the literature on seismic performance evaluation of RAC structures. Both the RAC and NAC were prepared and tested, from which their basic material properties were measured and compared. The smart aggregates made of cement modules enclosing the PZT patches were fabricated, and they were embedded in concrete beams to detect damage (created by saw-cut cracks with different depths) and monitor health condition (conditioned by the accelerated F/T cyclic process) of the RAC and NAC materials. The corresponding damage (crack) detection and condition assessment/monitoring techniques based on the wave propagation were developed and implemented. It demonstrated that the proposed damage detection technique is capable of capturing the existence and roughly the extent of the damage and the health monitoring technique is able to measure/monitor the degradable change of MOE due to the F/T conditioning.

## CONCLUSIONS

Based on the experimental evaluation of RAC and NAC samples and implementation of smart aggregates in damage detection and health monitoring of RAC beams conducted in this study, the following preliminary conclusions are obtained.

1. Based on the results from the mechanical property tests, RAC exhibits a lower compressive strength and MOE than those of NAC, although both types of concrete specimens meet the WSDOT 28-days compressive strength requirement of 4,000 psi (27.579 MPa). RAC also has a lower flexural strength than that of NAC.
2. During the concrete curing stage, the dynamic modulus of elasticity (MOE) values of RAC are lower than those of NAC, due to the lower mechanical property of the recycled aggregates (RA).
3. The dynamic MOE decreases for both NAC and RAC with the increase of the F/T cycles, and the degradation rates in NAC and RAC are comparable. Though RAC shows a low degradation (dynamic MOE reduction) percentage at the $300^{th}$ cycle, it tends to degrade at the higher rate than NAC after 180 F/T cycles, as reflected by the steeper slope of relative dynamic MOE.
4. The damage detection technique using embedded smart aggregates show its capability of detecting the severity of crack damage in concrete beams. The signal energy of the $1^{st}$ shear wave package can be used as an index to indicate the existence and approximately the extent of the crack damage.
5. The health monitoring technique using embedded smart aggregates also exhibits its capability of *in situ* assessing the change of MOE (aging or degradation) due to the F/T conditioning cycles in the concrete beams. The normalized MOE obtained for the wave propagation test decreases as the number of F/T cycles increases, demonstrating that both the RAC and NAC sample degrade with the F/T conditioning cycles. Again, the degradation (i.e., MOE reduction) trend

concluded from the wave propagation test is consistent with that from the dynamic modulus test based on the frequency measurement. Though RAC shows a low degradation (reduction of the wave propagation-based MOE) percentage at the 300$^{th}$ cycle, it tends to degrade at the higher rate than NAC after 180 F/T cycles, as reflected by the steeper slope of normalized MOE from the wave propagation test. The embedded smart piezoelectric aggregates and associated wave propagation-based health monitoring technique show their capability in assessing the degradation process in the RAC beams.

6. The degradation rates of both the RAC and NAC beams monitored by the proposed wave propagation test and embedded smart aggregate are consistent with those measured by the dynamic MOE test (ASTM C215). Though in general the mechanical performance of RAC is lower than that of its NAC counterpart, their material properties are comparable. The RAC (with coarse aggregates of 70% RA and 30% NA) considered in this study has the potential for widespread application in transportation construction.

## RECOMMENDATIONS

Based on the experimental program conducted and the damage detection and health monitoring techniques developed in this study, the following recommendations are suggested for promoting application of recycled aggregate concrete (RAC) in transportation construction and providing viable and effective damage detection and health monitoring techniques for concrete structures in general.

1. Though it is anticipated that the mechanical and durability properties of RAC are generally lower than those of NAC, RAC is comparable to NAC and thus

recommended for the use in the transportation construction as long as their basic material properties meet the minimum requirements.

2. The long term performance of RAC should be monitored, using either the conventional dynamic MOE test (ASTM C215) or the proposed smart health monitoring technique with embedded smart aggregates which is capable of *in situ* assessing the condition of the structures.
3. There are limited or no studies in assessing seismic performance of structures made of RAC. The preliminary study on seismic performance of lab-scale bridge models (e.g., as proposed in the Phase II study of this project) should be conducted, coupled with the implementation of damage detection and smart health monitoring techniques developed in this Phase I study.

## ACKNOWLEDGEMENTS

This research was partially supported by the Transportation Northwest (TransNow Regional Center)/USDOT and Washington State Department of Transportation (WSDOT). The recycled aggregates used in this study were donated by Central Pre-Mix Concrete Co. of Spokane, WA (Craig L. Matteson), and their generosity is gratefully acknowledged. The contributions to this research by the doctoral students Fan Wei and Fangliang Chen at WSU are very much appreciated.

## REFERENCES

Ajdukiewicz, A. and Kliszczewicz, A. (2002). "Influence of recycled aggregates on mechanical properties of HS/HPC," *Cement and Concrete Composites*, 24(2):69-79.

Ajdukiewicz, A.B. and Kliszczewicz, A.T. (2007). “Comparative tests of beams and columns made of recycled aggregate concrete and natural aggregate concrete,” *Journal of Advanced Concrete Technology*, 5(2):259-273.

BCSJ (1978). “Study on recycled aggregate and recycled aggregate concrete,” Building Contractors Society of Japan, Committee on Disposal and Reuse of Concrete Construction Waste, *Summary in Concrete Journal*, Japan, 16(7): 18-31 (in Japanese).

Brito, J., Pereira, A.S., and Correia, J.R. (2005). “Mechanical behavior of non-structural concrete made with recycled ceramic aggregates,” *Cement and Concrete Composites*, 27: 429-433.

Buyle-Bodin, F. and Hadjieva-Zaharieva, R. (2002). “Influence of industrially produced recycled aggregates on flow properties of concrete,” *Materials and Structures*, 35(8): 504-509.

Corinaldesi, V. and Moriconi, G. (2006). “Behavior of beam-column joints made of sustainable concrete under cyclic loading,” *Journal of Materials in Civil Engineering*, ASCE, Sep.-Oct.2006. pp.650-658.

Domingo-Cabo, A., Lázaro, C., López-Gayarre, F., et al. (2009). “Creep and shrinkage of recycled aggregate concrete,” *Construction and Building Materials*, 23(7): 2545-2553.

Frondistou-Yannas, S. (1977). “Waste concrete as aggregate for new concrete,” *Journal Proceedings, JL74-37*, 74(8): 373-376.

Gómez-Soberón, J. M. V. (2002). “Porosity of recycled concrete with substitution of recycled concrete aggregate: An experimental study,” *Cement and Concrete Research*, 32(8): 1301-1311.

Hansen, T.C. and Narud, H. (1983). “Strength of recycled concrete made from crushed concrete coarse aggregate,” *Concrete International*, 5(1):79-83.

Hansen, T.C. and Boegh, E. (1985). “Elasticity and drying shrinkage of recycled aggregate concrete,” *ACI Journal*, Sep-Oct, pp.648-652.

Hasaba, S., et.al. (1981). “Drying shrinkage and durability of concrete made of recycled concrete,” *Transition of the Japan Concrete Institute*, 3:55-60.

Hiroshi, T, Atsushi, N., et al. (2001). “High quality recycled aggregate concrete (HiRCA) processed by decompression and rapid release,” *ACI Special Publications*, Rep. No. SP-200, American Concrete Institute (ACI), Detroit, pp. 491–502.

Katz, A. (2003). "Properties of concrete made with recycled aggregate from partially hydrated old concrete," *Cement and Concrete Research*, 33: 703-711.

Kelly, T. (1998). "Crushed cement concrete substitution for construction aggregates-a materials flow analysis," *U.S. Geological Survey Circular 1177*, pp. 2.

Kosmatka, S.H., Kerkhoff, B., and Panarese, W.C. (2002). *Design and Control of Concrete Mixtures*, Portland Cement Association, pp. ix.

Kreijger, P.C. et al. (1987). "Ecological properties of building materials," *Materials and Structures*, 20(4): 248-254.

Levy, S.M. and Helene, P. (2004). "Durability of recycled aggregates concrete: a safe way to sustainable development," *Cement and Concrete Research*, 34:1975–1980.

Limbachiya, M. C., Leelawat, T. and Dhir, R.K. (2000). "Use of recycled concrete aggregate in high-strength concrete," *Materials and Structures*, 33(9): 574-580.

López-Gayarrea, F., Sernab, P., Domingo-Cabob, A., et al. (2009). "Influence of recycled aggregate quality and proportioning criteria on recycled concrete properties," *Waste Management*, 29(12): 3022-3028.

Luo, H. and Hanagud, S. (1999). "PVDF sensor and its applications in the delamination response detection," *Journal of Aerospace Engineering*, ASCE, 12(1), 23-30.

Malhotra, V.M. and Carino, N.J. (2004) "Handbook on nondestructive testing of concrete." Florida: CRC Press.

Metha, P.K. (1999). "Advancements in concrete technology," *Concrete International*, 6:69-76.

Nilsen, A.U. and Monteiro, P.J.M. (1993). "Concrete: A three phase material," *Cement and Concrete Research*, 23(1):147-151.

Nixon, P. J. (1978). "Recycled concrete as an aggregate for concrete - A review," *Materials and Structures*, 11(6), 371-378.

Oikonomou, N.D. (2005). "Recycled concrete aggregates," *Cement and Concrete Composites*, 27: 315–318.

Park, S., Ahmad, S., Yun, C.-B., and Roh, Y. (2006). "Multiple crack detection of concrete structures using impedance-based structural health monitoring techniques," *Experimental Mechanics*, 46: 609–618.

Poon, C.S. and Chan, D. (2006). "Paving blocks made with recycled concrete aggregate and crushed clay brick," *Construction and Building Materials*, 20(8):569-577.

Ravindrarajah, S. and Tam, R. (1985). “Properties of concrete made with crushed concrete as coarse aggregate,” *Magazine of Concrete Research*, 37(130): 29-38.

Ridzuan, A.R.M. et al. (2001). “The influence of recycled aggregate concrete on early compressive strength and drying shrinkage of concrete,” *Proceeding of the International Conference on Structural Engineering, Mechanics and Computation*, Cape Town, South Africa, pp.1415-1421.

Rogoff, M.J. and Williams, J.F. (1994). *Approaches to Implementing Solid Waste Recycling Facilities*. Noyes Publications.

Ryu, J.S. (2002). “Improvement on strength and impermeability of recycled concrete made from crushed concrete coarse aggregate,” *Journal of Material Science Letters*, 21:1565-1567.

Salem, R. M. (1996). *Strength and Durability Characteristics of Recycled Aggregate Concrete*. PhD Dissertation, University of Tennessee, Knoxville, TN.

Salem, R.M., Burdette, E.G., and Jackson, N.M. (2003). “Resistance to freezing and thawing of recycled aggregate concrete,” *ACI Materials Journal*, May-June, pp.216-221.

Sato, R., Maruyama, I., et al. (2007). “Flexural behavior of reinforced recycled concrete beams,” *Journal of Advanced Concrete Technology*, 5(1):43-61.

Shin, S.W., Qureshi, A.R., Lee, J.Y., et al. (2008). “Piezoelectric sensor based nondestructive active monitoring of strength gain in concrete,” *Smart Materials and Structures*, 17(5).

Sogo, M., Sogabe, T., Maruyama, I., et al. (2004). “Shear behavior of reinforced recycled concrete beams,” *Conference on the Use of Recycled Materials in Building and Structures*, Nov. 2004, Barcelona, Spain.

Soh, C.K., Tseng, K.K.H., Bhalla, S., et al. (2000). “Performance of smart piezoceramic patches in health monitoring of a RC bridge,” *Smart Materials and Structures*, 9(4):533-542.

Song, G., Mo, Y.L., Otero, K., et al. (2006). “Health monitoring and rehabilitation of a concrete structure using intelligent materials,” *Smart Materials and Structures*, 15(2): 309-314.

Song, G.B., Gu, H.C., and Mo, Y.L. (2008). “Smart aggregates: multi-functional sensors for concrete structures - a tutorial and a review,” *Smart Materials and Structures*, 17(3).

Sun, M.Q., Staszewski, W.J., Swamy, R.N., et al. (2008). "Application of low-profile piezoceramic transducers for health monitoring of concrete structures," *NDT & E International*, 41(8):589-595.

Tavakoli, M. and Soroushian, P. (1996). "Strengths of recycled aggregate concrete made using field-demolished concrete as aggregate," *ACI Materials Journal*, 93(2):178-181.

Topcu, I.B. and Sengel, S. (2004). "Properties of concretes produced with waste concrete aggregate," *Cement and Concrete Research*, 34: 1307–1312.

Tseng, K.K. and Wang, L. (2004). "Smart piezoelectric transducers for in situ health monitoring of concrete," *Smart Materials and Structures*, 2004.13(5):1017-1024.

Wen, Y.M., Chen, Y., Li, P., et al. (2007). "Smart concrete with embedded piezoelectric devices: Implementation and characterization," *Journal of Intelligent Material Systems and Structures*, 18(3): 265-274.

Wu, F. and Chang, F.-K. (2006a). "Debond detection using embedded piezoelectric elements in reinforced concrete structures – Part I: Experiment," *Structure Health Monitoring*, 5:5-15.

Wu, F. and Chang, F.-K. (2006b). "Debond detection using embedded piezoelectric elements for reinforced concrete structures – Part II: Analysis and algorithm," *Structure Health Monitoring*, 5:17-28.

Xiao, J.Z., Li, J.B., and Zhang, C. (2005). "Mechanical properties of recycled aggregate concrete under uniaxial loading," *Cement and Concrete Research*, 35:1187-1194.

Xiao, J.Z., Li, J.B., and Zhang, C. (2006). "On relationships between the mechanical properties of recycled aggregate concrete: An overview," *Materials and Structures*, 39:655-664.

Xiao, J.Z., Sun, J.D. and Falkner, H. (2006). "Seismic performance of frame structures with recycled aggregate concrete," *Engineering Structures*, 28:1–8.

Yan, S., Sun, W., Song, G.B., et al. (2009). "Health monitoring of reinforced concrete shear walls using smart aggregates," *Smart Materials and Structures*, 18(4).

Yang, Y.F. and Han, L.H. (2006). "Experimental behavior of recycled aggregate concrete filled steel tubular columns," *Journal of Constructional Steel Research*, 62:1310–1324.

Yang, Y.W., Hu, Y.H., and Lu, Y. (2008). "Sensitivity of PZT impedance sensors for damage detection of concrete structures," *Sensors*, 8(1):327-346.

Yoda, K. and Yoshikane, T. (1988). “Recycled cement and recycled in Japan,” *Proceedings of Second International RILEM Symposium on Demolition and Ruse of Concrete and Masonry*, Tokyo, Japan, pp.527-536.

Zaharieva, R., Buyle-Bodin, F. and Wirquin, E. (2004). “Frost resistance of recycled aggregate concrete,” *Cement and Concrete Research*, 34:1927-1932.

Zou, Y., Tong, L. and Steven, G.P. (2000). “Vibration-based model-dependent damage (delamination) identification and health monitoring for composites structures - A review,” *Journal of Sound and Vibration*, 230(2), 357-378.